


Inhibition of integrin $\alpha v \beta 6$ sparks T-cell antitumor response and enhances immune checkpoint blockade therapy in colorectal cancer

Philipp Busenhardt ¹, Ana Montalban-Arques,¹ Egle Katkeviciute,¹ Yasser Morsy,¹ Chiara Van Passen,² Larissa Hering,¹ Kirstin Atrott,¹ Silvia Lang,¹ Jesus Francisco Glaus Garzon,³ Elisabeth Naschberger,² Arndt Hartmann,⁴ Gerhard Rogler,¹ Michael Stürzl,² Marianne Rebecca Spalinger,¹ Michael Scharl¹

To cite: Busenhardt P, Montalban-Arques A, Katkeviciute E, *et al.* Inhibition of integrin $\alpha v \beta 6$ sparks T-cell antitumor response and enhances immune checkpoint blockade therapy in colorectal cancer. *Journal for ImmunoTherapy of Cancer* 2022;**10**:e003465. doi:10.1136/jitc-2021-003465

► Additional supplemental material is published online only. To view, please visit the journal online (<http://dx.doi.org/10.1136/jitc-2021-003465>).

Accepted 31 December 2021



© Author(s) (or their employer(s)) 2022. Re-use permitted under CC BY-NC. No commercial re-use. See rights and permissions. Published by BMJ.

For numbered affiliations see end of article.

Correspondence to

Professor Michael Scharl;
michael.scharl@usz.ch

ABSTRACT

Background Integrin $\alpha v \beta 6$ is a heterodimeric cell surface protein whose cellular expression is determined by the availability of the integrin $\beta 6$ subunit (ITGB6). It is expressed at very low levels in most organs during tissue homeostasis but shows highly upregulated expression during the process of tumorigenesis in many cancers of epithelial origin. Notably, enhanced expression of integrin $\alpha v \beta 6$ is associated with aggressive disease and poor prognosis in numerous carcinoma entities. Integrin $\alpha v \beta 6$ is one of the major physiological activators of transforming growth factor- β (TGF- β), which has been shown to inhibit the antitumor T-cell response and cause resistance to immunotherapy in mouse models of colorectal and mammary cancer. In this study, we investigated the effect of ITGB6 expression and antibody-mediated integrin $\alpha v \beta 6$ inhibition on the tumor immune response in colorectal cancer.

Methods Using orthotopic and heterotopic tumor cell injection, we assessed the effect of ITGB6 on tumor growth and tumor immune response in wild type mice, mice with defective TGF- β signaling, and mice treated with anti-integrin $\alpha v \beta 6$ antibodies. To examine the effect of ITGB6 in human colorectal cancer, we analyzed RNAseq data from the colon adenocarcinoma dataset of The Cancer Genome Atlas (TCGA-COAD).

Results We demonstrate that expression of ITGB6 is an immune evasion strategy in colorectal cancer, causing inhibition of the antitumor immune response and resistance to immune checkpoint blockade therapy by activating latent TGF- β . Antibody-mediated inhibition of integrin $\alpha v \beta 6$ sparked a potent cytotoxic T-cell response and overcame resistance to programmed cell death protein 1 (PD-1) blockade therapy in ITGB6 expressing tumors, provoking a drastic increase in anti-PD-1 treatment efficacy. Further, we show that the majority of tumors in patients with colorectal cancer express sufficient *ITGB6* to provoke inhibition of the cytotoxic T-cell response, indicating that most patients could benefit from integrin $\alpha v \beta 6$ blockade therapy.

Conclusions These findings propose inhibition of integrin $\alpha v \beta 6$ as a promising new therapy for colorectal cancer, which blocks tumor-promoting TGF- β activation, prevents

tumor exclusion of cytotoxic T-cells and enhances the efficacy of immune checkpoint blockade therapy.

BACKGROUND

The cell surface receptor integrin $\alpha v \beta 6$ is expressed exclusively in epithelial cells. While its expression is minimal in most healthy epithelia, it is highly upregulated during carcinogenesis of many epithelial cancers.^{1–3} Expression of integrin $\alpha v \beta 6$ correlates with decreased survival in numerous carcinomas, such as colorectal cancer (CRC),^{4–5} breast cancer,⁶ pancreatic ductal adenocarcinoma⁷ non-small cell lung cancer,⁸ cervical squamous cell carcinoma⁹ and others.^{1,2} Integrins are heterodimeric transmembrane receptors consisting of α and β subunits. The rate-limiting factor for the formation of the $\alpha v \beta 6$ heterodimer is the availability of the subunit integrin $\beta 6$ (ITGB6), which can only form a receptor complex together with the αv integrin subunit (ITGAV).¹⁰

A key function of integrin $\alpha v \beta 6$ is the activation of transforming growth factor- β (TGF- β).² In fact, integrin $\alpha v \beta 6$, together with integrin $\alpha v \beta 8$, are the major activators of TGF- β in vivo.¹¹ TGF- β is sequestered in the extracellular matrix (ECM) as a latent compound, which is formed by TGF- β , latency-associated peptide (LAP) and latent TGF- β binding proteins, forming the large latent complex (LLC). The concentration of TGF- β stored within the ECM in its latent form is several orders of magnitude higher than required to produce potent biological effects. Thus, TGF- β signaling is predominantly regulated by activation of latent TGF- β .¹¹ Within the TGF- β family, integrin $\alpha v \beta 6$ activates TGF- $\beta 1$, the most abundant and most commonly dysregulated isoform of

TGF- β in cancer, and TGF- β 3.¹¹ TGF- β activation through integrin α v β 6 occurs by binding of the RGD (Arg-Gly-Asp) peptide present in LAP that causes a conformational change in the LLC, which leads to the release of TGF- β from the LLC.^{1 2 10 11} Activated TGF- β can then bind to TGF- β type 2 receptor (TGFBR2), which recruits, transphosphorylates and activates TGF- β type 1 receptor (TGFBR1). Activated TGFBR1 phosphorylates the transcription factors SMAD2 and SMAD3, which subsequently translocate into the nucleus and modulate the expression of target genes together with other transcription cofactors.^{11–13}

TGF- β signaling inhibits T-cell proliferation and effector functions as well as T-cell differentiation into the Th1 subtype, which mediates prominent and well-characterized T cell responses against cancers. Additionally, TGF- β directly inhibits the cytotoxic program of CD8+ T cells by repressing the expression of several genes involved in their lytic function, such as perforin, granzyme A and B, and interferon-gamma (IFN- γ).^{12 13} In mouse models of colorectal and breast cancer, TGF- β inhibition promotes infiltration of T-cells into the tumor and causes a potent cytotoxic T-cell response against tumor cells.^{14 15} Further, tumors that are resistant to anti-PD-L1 immune checkpoint blockade therapy (CBT) are rendered susceptible by combining this treatment with TGF- β inhibition. This combination treatment provokes a vigorous antitumor immunity and tumor regression.^{14 15} A recent study showed that selective inhibition of TGF- β 1 activation is sufficient to overcome CBT resistance and to induce a profound antitumor response when combined with anti-programmed cell death protein 1 (PD-1) treatment.¹⁶ However, TGF- β signaling is involved in many physiological processes; thus, suppression of this pathway may lead to harmful off-target effects. Continuous long-term blockade of TGF- β 1 signaling causes hemorrhagic lesions within the heart valves, as well as aortic aneurysms in rats and dogs.^{17–19} The promising results of targeting TGF- β in preclinical models are therefore contrasted by modest success in clinical trials, where it proved difficult to determine a safe and effective dose.²⁰ A more promising approach to inhibit TGF- β signaling in a clinical setting might therefore be the prevention of TGF- β activation by blocking integrin α v β 6. Since integrin α v β 6 is predominantly expressed during carcinogenesis,^{1 2} harmful off-target effects might be greatly reduced compared with direct and systemic TGF- β inhibition.

TGF- β activation through integrin α v β 6 has been shown to affect T-cell function in triple-negative breast cancer (TNBC) and in the gastrointestinal tract. In TNBC, integrin α v β 6 activates TGF- β , which upregulates one of its target genes SOX4 in the tumor cells, causing resistance to T cell-mediated cytotoxicity.²¹ In the small intestine, integrin α v β 6 regulates the retention of tissue-resident memory T-cells by activating TGF- β .²² These findings prompted us to investigate whether integrin α v β 6 is affecting the T-cell immune response in CRC.

We show that ITGB6 inhibits the T-cell antitumor response and strongly accelerates tumor growth in murine models of CRC. Moreover, anti-ITGB6 treatment rendered tumors susceptible to PD-1 blockade, which caused a potent immune reaction and tumor shrinkage. Finally, we demonstrate that ITGB6 inhibits the T-cell immune response in the majority of human CRC tumors. These findings suggest upregulation of ITGB6 as an immune evasion strategy of tumor cells leading to the reduced survival rates seen in patients with tumors expressing ITGB6. Combining CBTs with anti-ITGB6 treatment might therefore be a promising, safe approach to overcome immune evasion and to increase the treatment success of current immunotherapies in CRC.

METHODS

Study design

Appropriate group sizes were determined on the basis of our previous experience with the models. In general, experiments aimed to include five mice per group, which were randomly assigned to the different treatments. Endpoint was reached when tumors were over 1000 mm³ or 1 cm in length or when mice showed wounds at the site of injection or poor health. These animals were euthanized and excluded from the analysis. Treatments were randomly performed and cage locations randomly assigned during the course of the experiments. Investigators administering the treatments were not blinded. Investigators terminating the experiments and processing the samples were blinded. No data outliers were excluded.

Mice

C57BL/6JRj, BALB/c and BALB/c nude mice were purchased from Janvier Labs (France). CD4-dnTGFBR2 (stock number 005551) and C57BL/6J (control for CD4-dnTGFBR2) were purchased from The Jackson Laboratory (USA). All mice were kept in specific-pathogen-free conditions. C57BL/6JRj, BALB/c and BALB/c nude mice were females between 9 and 11 weeks old at the start of the experiment. CD4-dnTGFBR2 and C57BL/6J were 9 weeks old at the start of the experiment.

Cloning of expression vector and viral transduction

For the construction of the ITGB6 overexpression vector, ITGB6 gene was amplified from ITGB6 cDNA ORF Clone in Cloning Vector (Sino Biological: MG50097-M) and cloned into the expression vector pLenti CMV GFP Blast (659-1) (Addgene plasmid # 17445)²³ in place of GFP. Cloning, lentiviral transduction, western blot and co-immunoprecipitation (Co-IP) were performed according to standard procedures as described in the supplementary methods.

Tumor models and treatments

Tumor cells were suspended in cell culture medium mixed 1:1 with matrigel (Corning 354263) and injected into the cecum wall (orthotopic model) or subcutaneously

into the flanks of the mice (heterotopic model) as described in detail in the supplementary methods. In the orthotopic model, mice were euthanized ~2 weeks after injection. In the subcutaneous model, tumor development was measured three times per week using a digital caliper. Tumor volume was calculated using the ellipsoid formula: $4/3 \times 3.14 \times \text{Length}/2 \times (\text{Width}/2)^2$,² where the shorter dimension was used as width and depth. Mice were terminated 14 days after subcutaneous injection. RT-qPCR analysis and histological staining and analysis of the tumor tissue were performed according to standard procedures as described in the supplementary methods.

$\alpha\beta6$ blockade was performed by injecting 4 mg/kg anti- $\alpha\beta6$ antibody (Biogen; 6.8G6 or Biogen; 6.3G9)²⁴ i.p. three times per week. All mice within one experiment received either anti- $\alpha\beta6$ antibody or the same amount of IgG isotype control antibody (Biogen; 1E6). PD-1 blockade was performed by injecting 10 mg/kg anti-PD1 (CD279) antibody (BioXCell; clone 29F.1A12) i.p. three times per week. All mice within one experiment received either anti-PD1 antibody or the same amount of IgG isotype control antibody (BioXCell; clone 2A3). 5-Fluorouracil (5-FU) was administered by i.p. injections of 50 mg/kg 5-FU dissolved in dimethyl sulfoxide (DMSO) at days 6, 9, and 12 after tumor cell injection. All mice within one experiment received either 5-FU treatment or the same amount of DMSO as vehicle control.

Flow cytometry

Spleen, lymph node (LN) and tumor cells were used for flow cytometry analysis. Single cell suspensions from spleen and LN were prepared as described previously.²⁵ Cecum and subcutaneous tumors were cut to approximately 0.5 mm³ pieces and digested in 6 mL RPMI medium containing 0.5 mg/mL collagenase type IV (Sigma Aldrich) and 0.05 mg/mL DNase I (Roche) solution for 10 min on a shaker (300 rpm) at 37°C. Cells were homogenized by passing the digested samples through a 18G1.5 syringe and centrifuged for 10 min, 4°C, 1500 rpm. Single cell suspensions were stained and restimulated as described previously.²⁶ A list of the used antibodies is given in online supplemental table 1.

RNAseq and data analysis

Subcutaneous MC38-ITGB6 and MC38-Ctrl tumors were used for RNAseq analysis. RNA isolation and sequencing were performed by Microsynth AG, Balgach, Switzerland. We used FastQC (V.0.11.5) to check the data quality, and mouse genome mm10 from Ensemble as a reference genome for STAR (V.2.5.4) for mapping the reads. The DESeq2 R package (V.1.28.1)²⁷ was used for detecting differentially expressed genes (DEGs). The negative binomial model and Wald test were performed together with Benjamini-Hochberg for multiple comparisons correction (false discovery rate (FDR) cut-off <0.05). A principal component analysis was performed across all the samples using the count of reads per kilobase per million mapped reads (RPKM). A heatmap was generated

from unsupervised clustering using DEGs. We used EnhancedVolcano R package (V.1.8.0) for the visualization of DEGs by volcano plot. Gene ontology (GO) was carried out using Database for Annotation, Visualization, and Integrated Discovery tool V.6.8.^{28 29} We used quantiseq software³⁰ to quantify different immune cell types. The deconvolution was based on the expression signature panel provided by the software. To summarize the signatures of T-TBRS and F-TBRS, Z-scores were computed for each gene and sample, averaged across all genes included in the profile. Signature differences between groups were assessed using Mann-Whitney tests.

Human sample collection and expression analysis

Expression analysis was conducted on tumor specimen of a prospectively collected cohort of patients with colon carcinoma who underwent surgery at the University Medical Center Erlangen. Clinical documentation was externally monitored in full. Exclusion criteria included preoperative radiation or chemotherapy, patients suffering from hereditary CRC (familial adenomatous polyposis, hereditary non-polyposis CRC) or inflammatory bowel disease (Crohn's disease, ulcerative colitis). RT-qPCR analysis and Immunohistochemical (IHC) staining of the human tumor specimen was performed as described in the supplementary methods.

Human RNAseq data analysis

The human gene expression dataset and the corresponding clinical data were retrieved from Genomic data commons data portal <https://portal.gdc.cancer.gov/>. The colon adenocarcinoma dataset from The Cancer Genome Atlas (TCGA-COAD) contains data from 521 patients with CRC grouped according to the tumor stage. The default trimmed mean of M-values implemented in EdgeR package (V.3.26.8)^{31 32} was used for gene counts normalization.

Statistics

When comparing two groups, unpaired two-tailed t-test was used. For human RNAseq data, Mann-Whitney test was used. For comparisons between three or more groups, one-way analysis of variance (ANOVA) was used and Tukey's post-hoc tests applied. Tumor growth curves were analyzed by two-way ANOVA and Tukey's post-hoc test. Statistics for DEG analysis of RNAseq are detailed above.

RESULTS

ITGB6 promotes tumor growth by inhibiting the T-cell antitumor immune response

To investigate the effect of ITGB6 on tumor development, we overexpressed ITGB6 in the two murine CRC cell lines CT26 and MC38, which present with low endogenous ITGB6 expression (figure 1A). ITGB6 overexpression was performed by viral transduction with an ITGB6-expressing vector (ITGB6) and control cells were

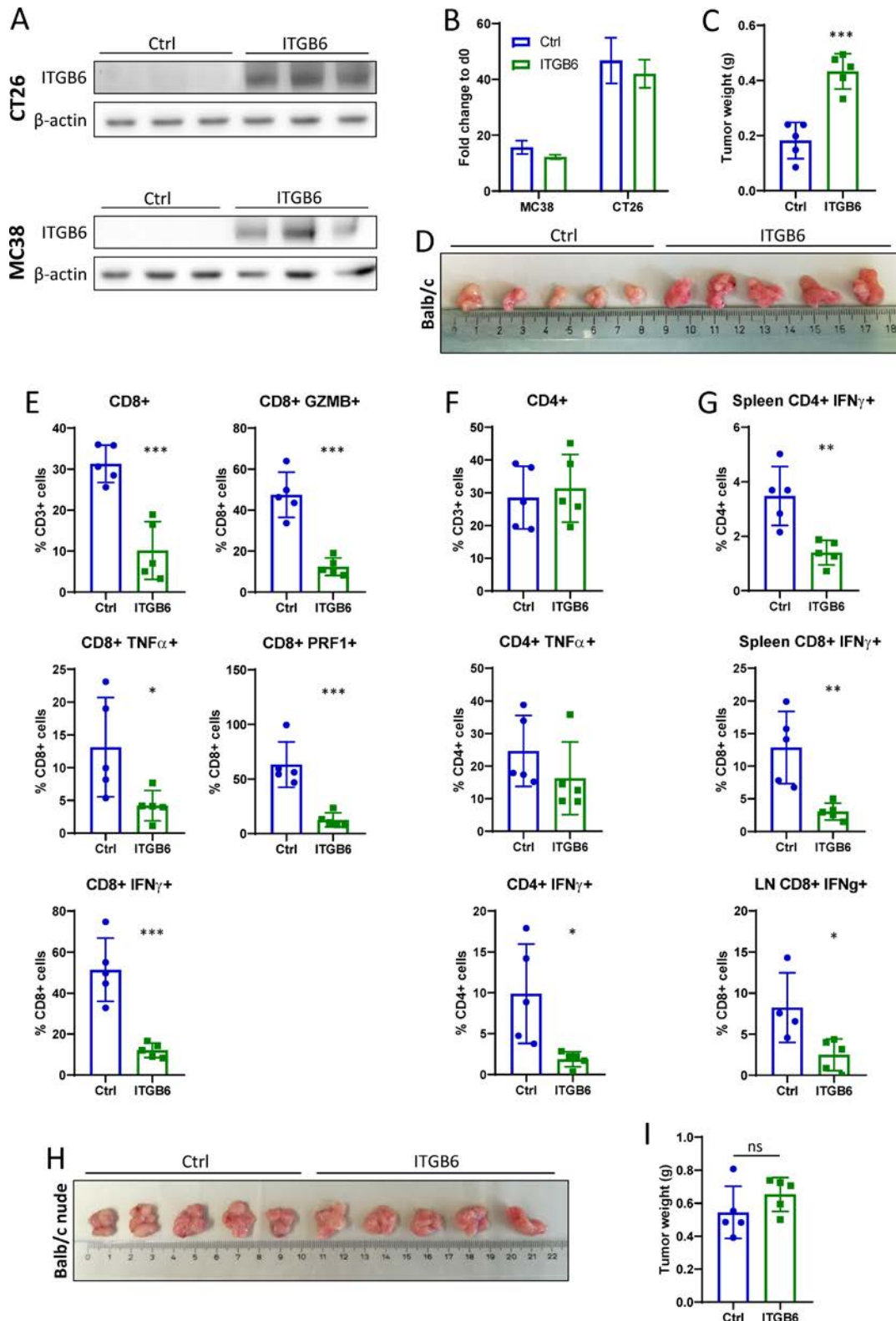


Figure 1 ITGB6 promotes tumor growth by inhibiting the T-cell antitumor immune response. (A) Western blot for ITGB6 in MC38 and CT26 cells that overexpress ITGB6. (B) 3-day proliferation assay with ITGB6 overexpressing and control cells. (C) CT26-ITGB6 and CT26-Ctrl ceceum tumors at day 13 after injection into Balb/c mice. (D) Weight of CT26-ITGB6 and CT26-Ctrl ceceum tumors at day 13 after injection. (E) Flow cytometry analysis of CD8+ T cells isolated from tumor. (F) Flow cytometry analysis of CD4+ T cells isolated from tumor. (G) Flow cytometry analysis of CD8+ and CD4+ T cells isolated from spleen and lymph node (LN). (H) CT26-ITGB6 and CT26-Ctrl ceceum tumors at day 13 after injection into Balb/c nude mice. (I) Weight of CT26-ITGB6 and CT26-Ctrl ceceum tumors at day 13 after injection into Balb/c nude mice. Means and SDs are shown (n=5 mice). Unpaired two-tailed t-test was used to calculate statistical significance. ns=not significant ($p \geq 0.05$), * $p < 0.05$, ** $p < 0.01$, *** $p < 0.001$, **** $p < 0.0001$.

transduced with an empty control vector (Ctrl). Co-IP of ITGB6 and ITGAV showed that the overexpressed ITGB6 is forming a heterodimer with endogenously expressed ITGAV (online supplemental figure S1B). Since ITGB6 expression has been reported to accelerate cell proliferation,^{33–35} we performed a 3-day proliferation assay in vitro to define the proliferation rate. However, neither CT26 nor MC38 cells showed upregulated proliferation on ITGB6 overexpression (figure 1B).

Next, to examine the effect of ITGB6 on intestinal tumor growth in vivo, we performed cecum injections of CT26-ITGB6 cells and CT26-Ctrl cells in Balb/c mice, which are syngeneic to the CT26 cell line. Mice injected with CT26-ITGB6 cells showed accelerated tumor growth, leading to larger and heavier tumors at the time of sacrifice (figure 1C,D). IHC stainings of the tumors for CD3, CD4, and CD8 showed significantly decreased T-cell numbers in ITGB6 tumors compared with Ctrl tumors whereas the proliferation marker Ki67 did not show any difference in tumor cell proliferation (online supplemental figure S1A). RT-qPCR analysis of the tumors revealed a massive upregulation of *Itgb6* expression in CT26-ITGB6 tumors, causing decreased gene expression of the inflammatory cytokines tumor necrosis factor α (*Tnfa*) and interferon γ (*Ifng*), the cytolytic enzymes granzyme B (*Gzmb*) and perforin (*Prf1*), as well as the Th1 marker T-bet (*Tbx21*) (online supplemental figure S1C). Analysis of the T-cell compartment in the tumors by flow cytometry showed that the proportion of CD8⁺ T cells was reduced by ITGB6 (figure 1E). Similarly, granzyme B, perforin, IFN- γ and TNF- α expression were strongly downregulated by ITGB6 in CD8⁺ T cells (figure 1E), whereas CD4⁺ T cells were not affected in their proportion, but showed reduced IFN- γ expression (figure 1F). ITGB6 also downregulated the expression of IFN- γ in CD8⁺ T cells isolated from spleen and draining LNs and in splenic CD4⁺ T cells (figure 1G). For further analysis of the effect of ITGB6 expression in the tumor, we performed subcutaneous tumor injections. CT26-ITGB6 and CT26-Ctrl cells were injected into Balb/c mice and MC38-ITGB6 and MC38-Ctrl cells were injected into C57BL/6 mice, which are syngeneic to MC38 cells. Analogous to orthotopic injections, mice with CT26-ITGB6 or MC38-ITGB6 tumors showed a strongly enhanced tumor growth compared with mice with CT26-Ctrl or MC38-Ctrl tumors (online supplemental figure S2A–C, E–G), as well as inhibition of the cytotoxic CD8⁺ T cell response. Inhibition of CD8⁺ T cell activation is indicated by decreased proportions of CD8⁺ cells within the CD3⁺ fraction and decreased expression of granzyme B, perforin, IFN- γ and TNF- α (online supplemental figure S2D,H). Similarly, CD4⁺ T cells showed decreased expression of IFN- γ and TNF- α (online supplemental figure S2D,H). Together with the inhibition of T-cell responses, gene expression of the chemokines CXCL9, CXCL10 and CXCL11, which are known to be involved in T-cell infiltration and activation as well as T-cell differentiation into the Th1 subtype,³⁶ was suppressed in subcutaneous CT26-ITGB6 tumors (online supplemental figure S3A).

These data demonstrate that ITGB6 inhibits T-cells and promotes tumor growth independently of the tumor location or genetic background of the host.

To confirm that the tumor growth promoting effect of ITGB6 is mediated by T-cell inhibition, we injected CT26-ITGB6 and CT26-Ctrl cells into Balb/c nude mice, which are lacking T-cells. In these mice, no significant difference in tumor weight was observed between CT26-ITGB6 and CT26-Ctrl tumors, indicating that tumor growth acceleration caused by ITGB6 is mediated by T-cell inhibition (figure 1H,I).

Cytotoxic immune response regulation is the main function of ITGB6 within the tumor

In order to obtain an overview over the functions of ITGB6 within the tumor, we performed RNA-seq transcriptomic analysis on subcutaneous MC38-ITGB6 and MC38-Ctrl tumors. Unsupervised hierarchical clustering of the observed DEGs grouped the biological replicates of MC38-ITGB6 and of MC38-Ctrl tumors into two distinct clusters (figure 2A). Many of the most significantly downregulated genes in MC38-ITGB6 tumors were T-cell markers (*CD3d*, *CD3e*, *CD3g*, *CD8a*, *Trbc1*, *Trbc2*) or genes involved in T-cell activation (*Cxcl9*, *Txk*, *Itk*) and cytotoxic functions (*Gzmb*, *Gzma*, *Prf1*) (figure 2B). We further investigated the function of the DEGs by GO enrichment analysis (figure 2C). The DEGs were mainly involved in biological processes related to the immune system and those were strongly downregulated in MC38-ITGB6 tumors, indicating a strong effect of ITGB6 on the immune response. Therefore, besides cell adhesion, which also appears as one of the most affected biological processes, the main function of ITGB6 in the tumor appears to be the modulation of immune responses. Since adaptive as well as innate immune responses seem to be affected (figure 2C), we aimed to define changes in the proportions of different immune cell types in the tumors. An established computational method, using cell type-specific gene expression references, was used to deconvolute these cell type proportions from the bulk tissue RNA-seq data. While monocytes and regulatory T-cells (T-regs) were unaffected, proportions of several immune cell types, such as NK cells, B cells, M2 macrophages and neutrophils, were mildly affected by ITGB6 expression (online supplemental figure S3B). However, the proportion of CD8 T-cells within the tumors was strongly downregulated by ITGB6 (online supplemental figure S3B). Therefore, the main effect of ITGB6 in the antitumor immune response is the regulation of the cytotoxic T-cell reaction.

T-cell inhibiting effect of ITGB6 is mediated through TGF- β activation

Phosphorylation of SMAD2 and SMAD3 was significantly upregulated in subcutaneous CT26-ITGB6 tumors compared with CT26-Ctrl tumors (figure 3A), demonstrating that integrin $\alpha\beta 6$ activates TGF- β signaling in the tumor. Likewise, analyzing our RNA-seq data for TGF- β

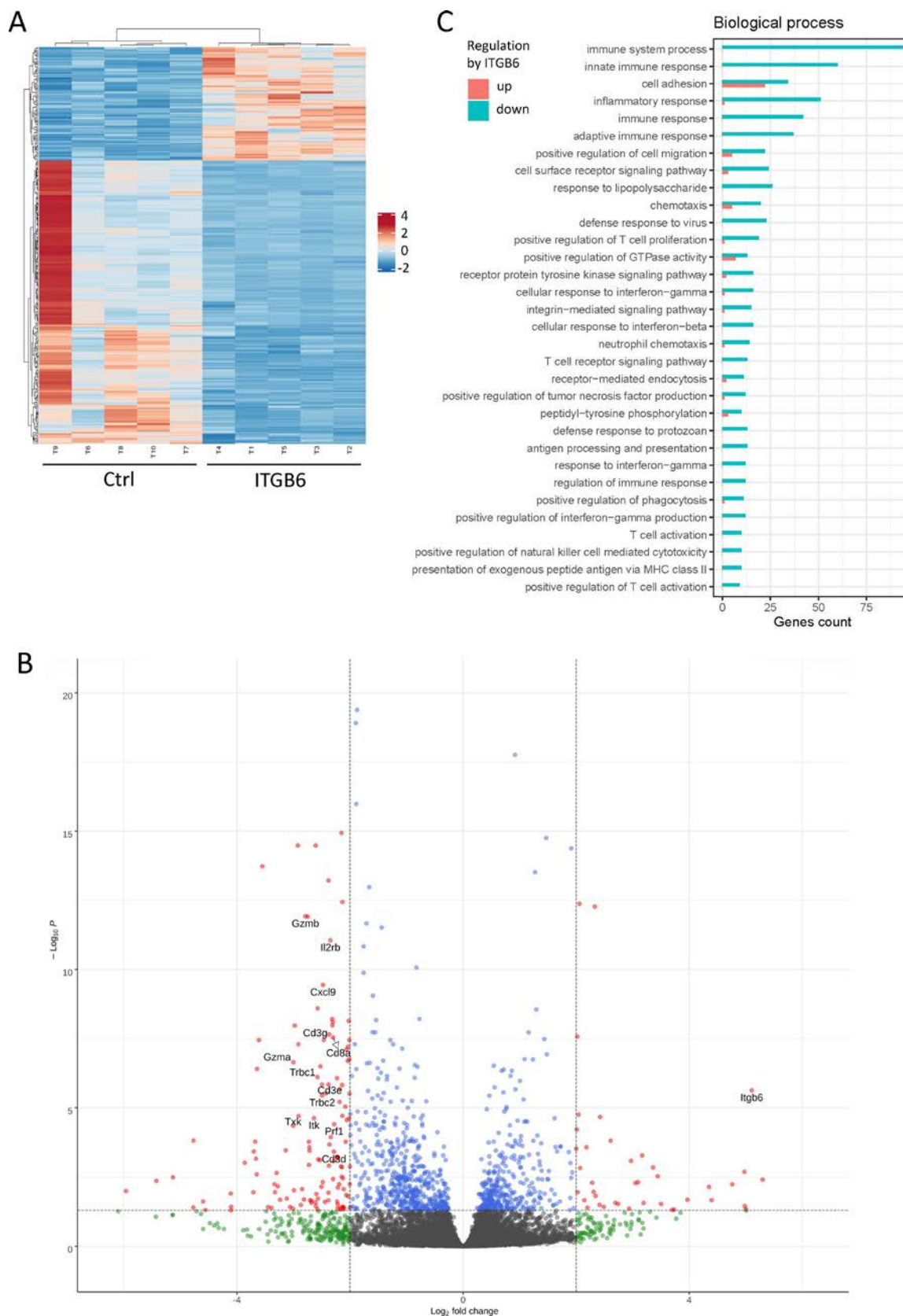


Figure 2 Cytotoxic immune response regulation is the main function of ITGB6 within the tumor. (A) Heatmap of differentially expressed genes (DEGs) ($p < 0.001$) in MC38-ITGB6 and MC38-Ctrl tumors, generated by unsupervised hierarchical clustering ($n = 5$ mice). (B) Volcano plot displaying DEGs from MC38-ITGB6 versus MC38-Ctrl tumors. Y-axis corresponds to p value of $-\log_{10}$. X-axis displays log₂-fold change value. Indicated limits represent DEGs with $p < 0.05$ and log₂ fold change above +2 or below -2. (C) Gene ontology enrichment analysis of DEGs. Bars in red or blue indicate the number of genes involved in upregulation or downregulation of the respective biological process in ITGB6-expressing tumors.

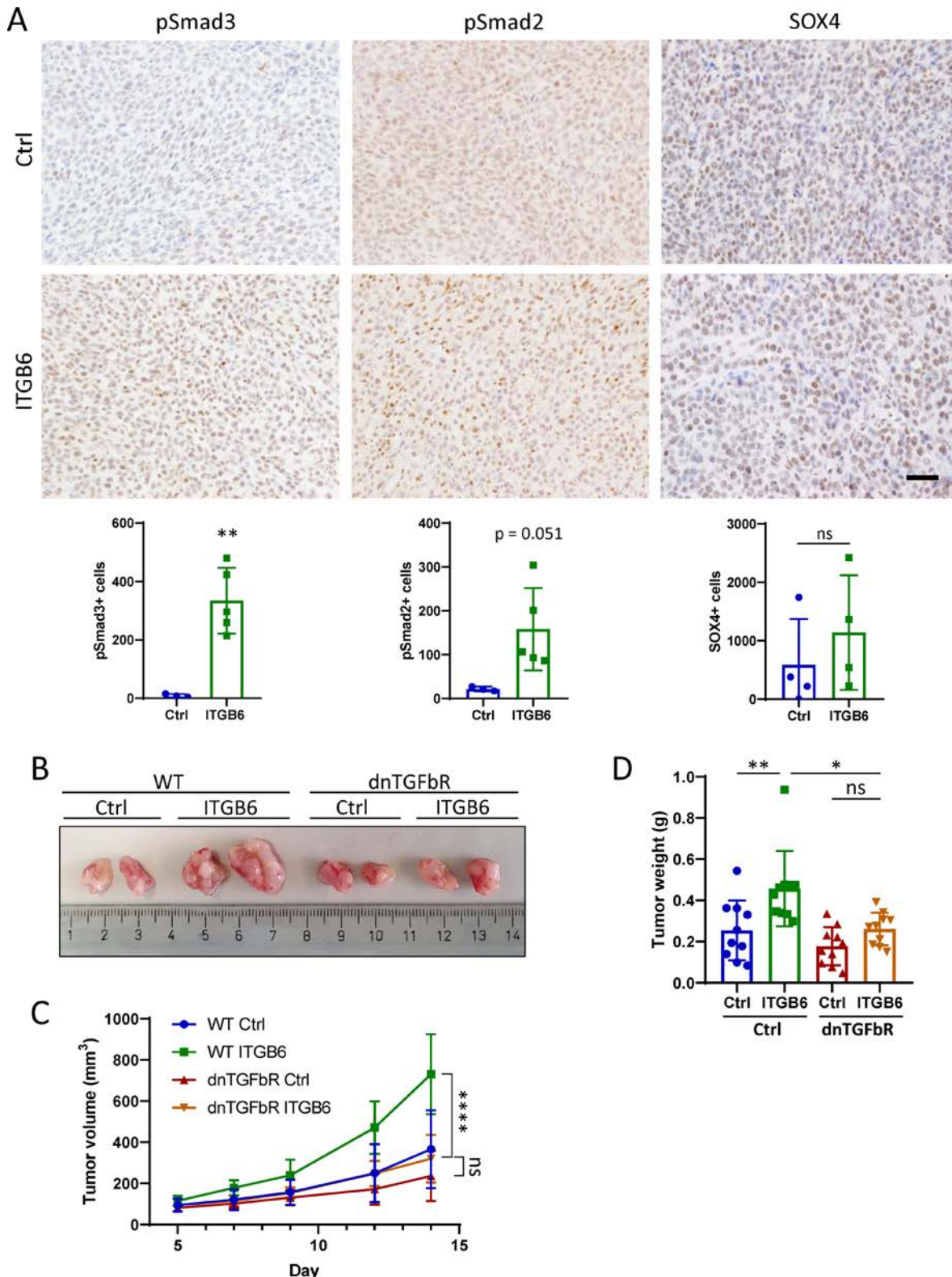


Figure 3 T-cell inhibiting effect of ITGB6 is mediated through TGF- β activation. (A) Immunohistochemical (IHC) stainings for pSmad2, pSmad3 and SOX4 in subcutaneous CT26-ITGB6 and CT26-Ctrl tumors. Representative images of IHC stainings (top) and quantification of the number of stained cells (below). Scale bar=50 μ m. (B) Representative image of subcutaneous CT26-ITGB6 and CT26-Ctrl tumors grown in CD4-dnTGFBR2 mice or C57BL/6 WT mice at day 14 after injection. (C) Tumor volume development of CT26-ITGB6 and CT26-Ctrl tumors grown in CD4-dnTGFBR2 mice or C57BL/6 WT mice. (D) Weight of CT26-ITGB6 and CT26-Ctrl tumors grown in CD4-dnTGFBR2 mice or C57BL/6 WT mice at day 14 after injection. Means and SDs are shown. Unpaired two-tailed t-test (A) (n=5 mice), one-way analysis of variance (ANOVA) (D) and two-way ANOVA (C) with Tukey's post-hoc test (n=5 mice, 2 tumors per mouse) were used to calculate statistical significance. ns=not significant ($p \geq 0.05$), * $p < 0.05$, ** $p < 0.01$, *** $p < 0.001$, **** $p < 0.0001$.

response signatures in fibroblasts (F-TBRS) and T-cells (T-TBRS)^{37,38} demonstrated increased levels of TGF- β signaling in MC38-ITGB6 tumors compared with MC38-Ctrl tumors (online supplemental figure S3C). We also observed an upregulation of CALD1 and IGFBP7, two TGF- β induced factors expressed in stromal cells of the tumor, which predict poor prognosis³⁸ (online supplemental figure S3D). However, we did not observe a significant upregulation of SOX4 (figure 3A), a TGF- β target gene that has been reported to inhibit the T-cell response when expressed by the tumor cells in TNBC.²¹ To further investigate the role of $\alpha\beta6$ -mediated TGF- β activation in the T-cell tumor response, we subcutaneously injected CT26-ITGB6 and CT26-Ctrl cells into CD4-dnTGFBR2 transgenic mice, which express a dominant-negative form of TGFBR2 selectively in CD4+ and CD8+ T cells. These transgenic mice exhibit blocked TGF- β signaling specifically and exclusively in CD4+ and CD8+ T cells.³⁹ In CD4-dnTGFBR2 mice, no difference in tumor weight or volume was observed between CT26-ITGB6 and CT26-Ctrl tumors, whereas in wildtype (WT) mice CT26-ITGB6 tumors showed significantly increased growth (figure 3B–D). Furthermore, CT26-ITGB6 tumors grew significantly larger in WT mice compared with the same tumors in CD4-dnTGFBR2 mice (figure 3B–D). Together, these results show that the tumor growth promoting and T-cell inhibiting effect of ITGB6 is mediated by increased TGF- β signaling in T-cells.

ITGB6 expression leads to local, but not systemic T-cell inhibition

T-cells isolated from spleens and LNs of mice bearing ITGB6 expressing tumors showed significantly decreased IFN- γ expression compared with the ones from mice with control tumors (figure 1G), suggesting that ITGB6 expression in the tumor might cause systemic T-cell inhibition. Therefore, we examined if T-cell inhibition provoked by ITGB6-tumors affects the growth of Ctrl tumors within the same host. For that purpose, we subcutaneously injected CT26-ITGB6 tumors in one flank and CT26-Ctrl tumors in the other flank of the same mouse and compared tumor growth and T-cell activity in these tumors to their respective counterparts in mice only bearing CT26-ITGB6 or CT26-Ctrl tumors (figure 4A). Tumor size of CT26-Ctrl tumors (Mix Ctrl) was not affected by the presence of CT26-ITGB6 tumors (figure 4B,C). Similarly, the CT26-ITGB6 tumors did not affect the CD8+ T cell proportion, cytotoxic activity, Th1 differentiation or T-cell infiltration in the CT26-Ctrl tumor (Mix Ctrl) in the same mouse (figure 4D, online supplemental figure S4). Likewise, the presence of CT26-Ctrl tumors and concomitant T-cell activation did not inhibit the growth or enhance T-cell infiltration or T-cell activity in CT26-ITGB6 tumors (Mix ITGB6) (figure 4B, online supplemental figure S4). Immunofluorescent staining from the boundary of CT26-ITGB6 tumors revealed that CD8+ T cells were mainly present outside the tumor mass where only little pSmad3 is detected and were not able to infiltrate into the tumor

tissue with more pSmad3 expression (figure 4E). These T-cells surrounding the tumor mass showed undetectable or very low pSmad3 staining (figure 4E). Very few CD8 T-cells were present in the center of these tumors and showed higher pSmad3 expression (figure 4E). These data indicate that CD8 T-cells are locally inactivated and blocked from infiltrating the tumor mass by direct TGF- β signaling in T-cells. Thus, systemically activated T-cells are ineffective against ITGB6-expressing tumors and T-cell inhibition through ITGB6 expression is acting only locally in ITGB6-expressing tumors and is not transmitted to tumors with low levels of ITGB6 expression. This creates a direct selective pressure that selects towards tumor cells with elevated expression of ITGB6, enabling them to escape the cytotoxic T-cell response.

Integrin $\alpha\beta6$ blockade sparks T-cell antitumor response and overcomes resistance to CBT

After demonstrating that expression of integrin $\alpha\beta6$ is an immune evasion strategy of tumor cells, we examined if integrin $\alpha\beta6$ can be effectively targeted to induce T-cell antitumor responses. For that purpose, we subcutaneously injected CT26-ITGB6 tumors and treated the mice with either the $\alpha\beta6$ neutralizing antibody 6.8G6 (α ITGB6) or isotype control antibody (IgG) (figure 5A). Tumor size was significantly decreased after treating the tumors with α ITGB6 for 12 days (figure 5B–D). Moreover, inhibition of $\alpha\beta6$ significantly increased the proportion of CD8+ T cells and the expression of the cytolytic enzymes granzyme B and perforin (figure 5E). Interestingly, α ITGB6 treatment also led to heavily increased expression of the immune checkpoint molecules CTLA-4 and PD-1 (figure 5E), suggesting that T-cell antitumor response might be further enhanced with CBT. Therefore, we combined α ITGB6 treatment with a PD-1 blocking antibody (α PD-1) in a subsequent experiment (figure 5F). Notably, ITGB6 expressing tumors seemed to be resistant to CBT since treatment with α PD-1 alone did not have any effect on tumor growth (figure 5G–I). However, while α ITGB6 treatment alone decreased tumor growth significantly, the combination with α PD-1 caused an even more potent immune response leading to tumor shrinkage (figure 5G–I). While there was no effect on the T-cell response by α PD-1 treatment alone (figure 5J), combination treatment triggered similar granzyme B, perforin and T-bet expression levels as α ITGB6 alone and the proportion of CD8+ T cells in the tumor was even further increased (figure 5J). CD4+ T cell proportion in the tumor was not affected by α ITGB6 or the combination treatment (figure 5J). Splenic CD8+ and CD4+ T cells showed elevated expression of IFN- γ and TNF- α as well as T-bet on α ITGB6 treatment, which was further enhanced in mice treated with α ITGB6 and α PD-1 (online supplemental figure S5A). Both treatment modalities also led to higher expression of the activation marker CD44 in splenic T-cells (online supplemental figure S5A). IHC staining of pSmad3, CD3, CD4 and CD8 revealed decreased TGF- β signaling and a higher abundance of

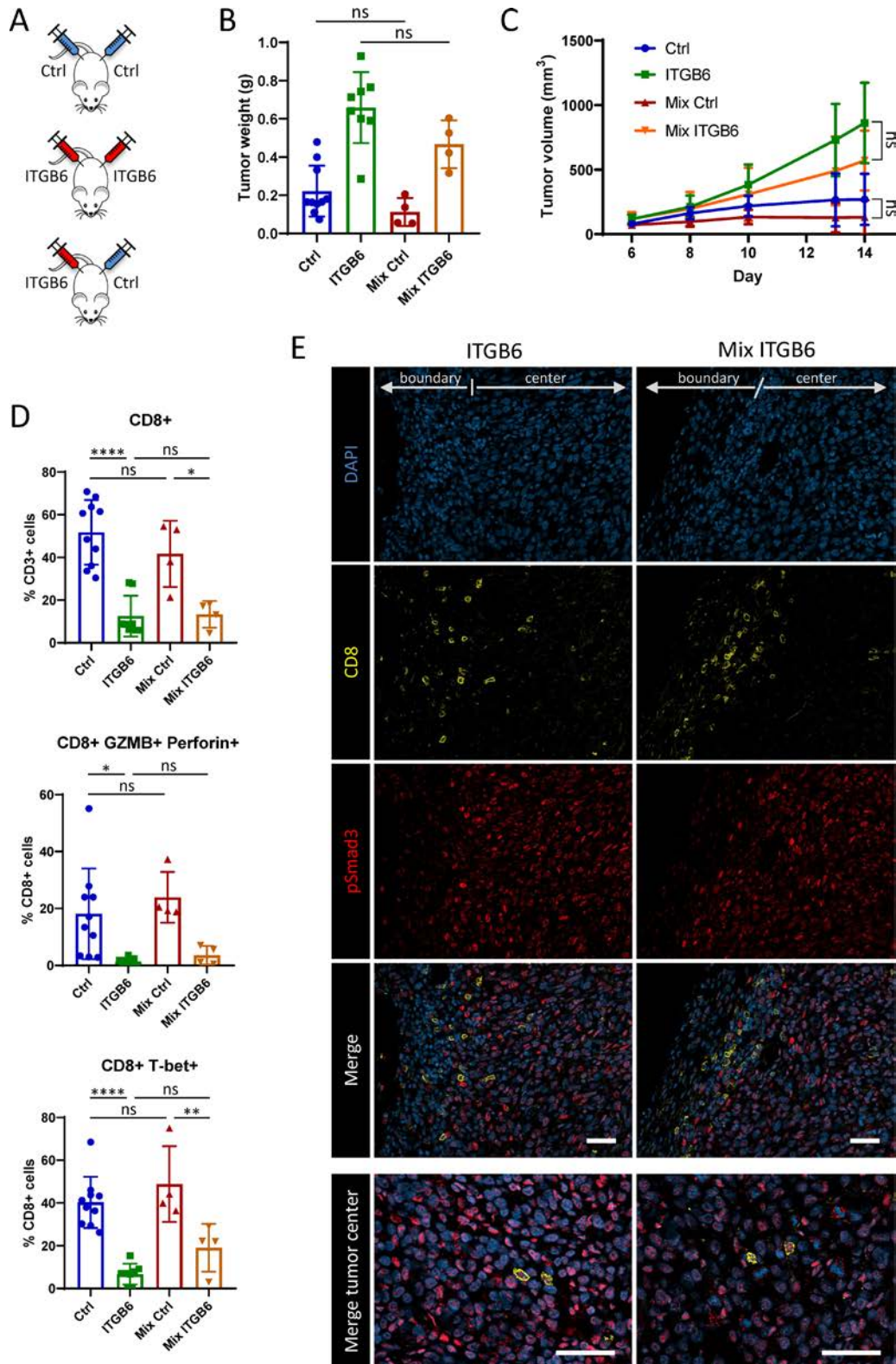


Figure 4 ITGB6 expression leads to local, but not systemic T-cell inhibition. (A) Experimental design of injection scheme. Subcutaneous injection of CT26-Ctrl tumors or CT26-ITGB6 tumors in both flanks or CT26-Ctrl tumors in one flank and CT26-ITGB6 tumors in the other flank of the mice (Mix). (B) Weight of tumors from mice bearing only CT26-ITGB6 or CT26-Ctrl tumors or mice bearing both tumors (Mix). (C) Tumor volume development of tumors from mice bearing only CT26-ITGB6 or CT26-Ctrl tumors or mice bearing both tumors (Mix). (D) Flow cytometry analysis of T-cells isolated from tumors of mice bearing only CT26-ITGB6 or CT26-Ctrl tumors or mice bearing both tumors (Mix). (E) Immunofluorescent stainings for CD8 and pSmad3 in CT26-ITGB6 tumors from mice bearing only CT26-ITGB6 tumors or mice bearing both tumors (Mix). Means and SDs are shown (n=5 mice). One-way analysis of variance (ANOVA) (B and D) and two-way ANOVA (C) with Tukey's post-hoc test were used to calculate statistical significance. ns=not significant ($p \geq 0.05$), * $p < 0.05$, ** $p < 0.01$, *** $p < 0.001$, **** $p < 0.0001$.

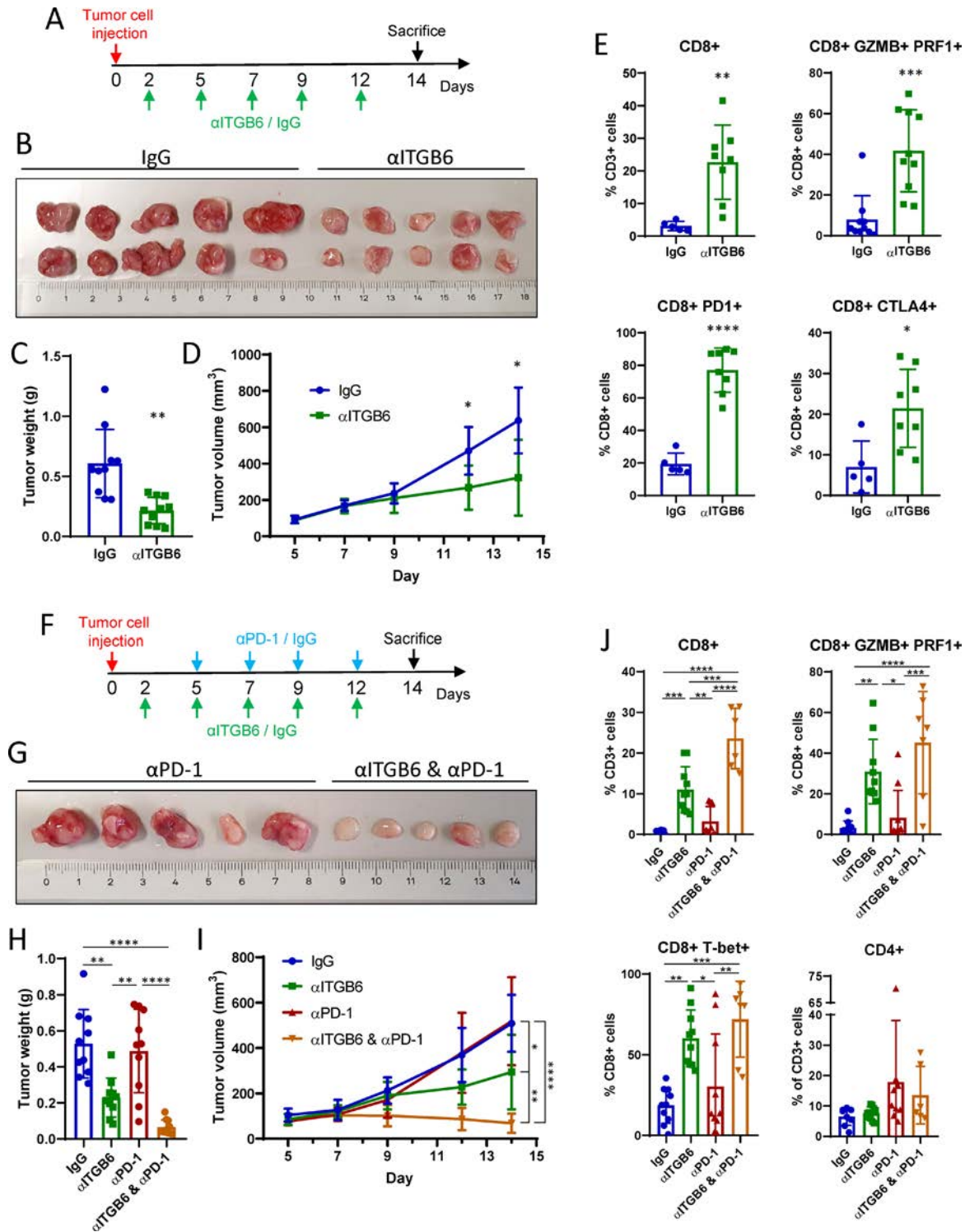


Figure 5 Integrin $\alpha\beta6$ blockade sparks T-cell antitumor response and overcomes resistance to CBT. (A) Experimental design of α ITGB6 antibody (6.8G6) administration. (B) Subcutaneous CT26-ITGB6 tumors treated with α ITGB6 or IgG control. (C) Tumor weight of subcutaneous CT26-ITGB6 tumors treated with α ITGB6 or IgG control. (D) Tumor volume development of subcutaneous CT26-ITGB6 tumors treated with α ITGB6 or IgG control. (E) Flow cytometry analysis of CD8⁺ T cells in CT26-ITGB6 tumors treated with α ITGB6 or IgG control. (F) Experimental design of α ITGB6 (6.8G6) and α PD-1 antibody administration. (G) Representative image of subcutaneous CT26-ITGB6 tumors treated with α PD-1 or α ITGB6 and α PD-1. (H) Tumor weight of subcutaneous CT26-ITGB6 tumors treated with α ITGB6, α PD-1, α ITGB6 and α PD-1 or IgG control. (I) Tumor volume development of subcutaneous CT26-ITGB6 tumors treated with α ITGB6, α PD-1, α ITGB6 and α PD-1 or IgG control. (J) Flow cytometry analysis of CD8⁺ T cells in CT26-ITGB6 tumors treated with α ITGB6, α PD-1, α ITGB6 and α PD-1 or IgG control antibody. Means and SDs are shown (n=5 mice, 2 tumors per mouse). Unpaired two-tailed t-test (C, E) one-way analysis of variance (ANOVA) (H, J) and two way ANOVA (D and I) with Tukey's post-hoc test were used to calculate statistical significance. *P<0.05, **p<0.01, ***p<0.001, ****p<0.0001.

CD8⁺ T cells in α ITGB6-treated tumors (online supplemental figure S5B, S6). Together, these data show that ITGB6 expression causes resistance to α PD-1 therapy, which can be overcome by combining CBT with α v β 6 blockade to provoke a potent T-cell antitumor response.

In a next step, we examined if α PD-1 therapy efficacy can also be improved with a different α v β 6-blocking antibody (6.3G9) to exclude that the antitumor effect is specific to the α ITGB6 antibody that we previously used (6.8G6) or specific to the epitope targeted by that antibody.²⁴ Differences in tumor size as well as cytotoxic CD8⁺ T cell activity showed the same additive effects of 6.3G9 together with α PD-1 therapy as observed before with 6.8G6 (online supplemental figure S7A–E). Additionally, staining for Ki67 in this experiment showed that α ITGB6 and α PD-1 combination treatment strongly enhances the proliferation of CD8⁺ T cells in the tumors (online supplemental figure S7E), which might partly explain the observed increase of CD8⁺ T cell numbers. In conclusion, α PD-1 therapy efficacy might be enhanced with any integrin α v β 6-inhibiting agent and is not antibody-dependent or epitope-dependent.

We further investigated whether the efficacy of the chemotherapeutic drug 5-FU, one of the most commonly used agents in CRC treatment,⁴⁰ can be enhanced by α ITGB6 (6.8G6) administration. For that purpose, we compared the effect of 5-FU or α ITGB6 administration alone to the combination of 5-FU and α ITGB6 in subcutaneous CT26-ITGB6 tumors (online supplemental figure S8A). All treatment modalities inhibited tumor growth with no significant differences between the three treatment groups (online supplemental figure S8A–D). Thus, in CT26-ITGB6 tumors, α ITGB6 is as efficient in controlling tumor growth as 5-FU, whereas the combination of them does not provoke an additive effect. The inability of α ITGB6 to enhance 5-FU treatment efficiency might be explained by the T-cell inhibiting effect of 5-FU administration. While CD8⁺ T cells are abundantly present and produce high amounts of granzyme B and perforin in the α ITGB6 treated group, this T-cell activating effect was eradicated on combination with 5-FU (online supplemental figure S8E). These data are in accordance with previous studies, which show that repeated 5-FU application impairs T-cell antitumor immune functions.⁴¹ Therefore, efficacy of α ITGB6 treatment, or any other T-cell activating therapy, might be impaired by combined administration with the chemotherapeutic drug 5-FU.

Integrin α v β 6 blockade overcomes resistance to CBT in tumors without artificial ITGB6 overexpression

So far, our data have demonstrated that combination treatment with α ITGB6 and α PD-1 is effective in ITGB6 overexpressing tumors with artificially enhanced ITGB6 expression levels. Whereas this model is useful to study the effects of ITGB6 on tumor growth and immune response, its vigorous ITGB6 expression cannot be compared with ITGB6 levels in tumors that naturally develop from somatic cells and upregulate ITGB6 expression through

a selective process. To find a model that resembles ITGB6 expression of a human tumor more closely, we assessed endogenous *Itgb6* expression in the murine mammary carcinoma cell line 4T1. The 4T1 cell line exhibited high endogenous *Itgb6* expression when compared with CT26 or MC38 cells, yet *Itgb6* expression in CT26-ITGB6 and MC38-ITGB6 cells was 150–300 times higher than in 4T1 cells (figure 6A). Similarly, when injected as subcutaneous tumors, 4T1 tumors expressed substantially less *Itgb6* than CT26-ITGB6 and MC38-ITGB6 tumors (figure 6B). We therefore examined the efficacy of the α ITGB6 (6.8G6) and α PD-1 combination treatment in subcutaneously injected 4T1 tumors (figure 6C). As seen before in ITGB6 overexpressing tumors, α PD-1 treatment alone did not have any effect on tumor growth, indicating that even a low level of ITGB6 expression is enough to confer CBT resistance (figure 6D,E). However, α v β 6 blockade overcame this resistance in 4T1 tumors and boosted α PD-1 therapy efficacy, leading to significantly reduced tumor size compared with isotype control IgG-treated tumors (figure 6D,E). Therefore, α ITGB6 and α PD-1 combination therapy is effective to treat tumors with moderate ITGB6 expression levels.

Integrin α v β 6 inhibits T-cell immune response in the majority of patients with CRC

Having shown that ITGB6 inhibits the T-cell antitumor response and accelerates tumor growth in mice, we investigated the effect of ITGB6 expression in human tumors. For that purpose, we analyzed *ITGB6* expression in tumor specimen of a prospectively collected cohort of 343 patients with colon carcinoma by RT-qPCR. Disease free survival was significantly decreased in patients with high *ITGB6* expression in the tumor, indicating that ITGB6 promotes a more aggressive disease course (figure 7A). IHC stainings of human CRC tumors with high or low *ITGB6* expression revealed that there is no association of SOX4 staining intensity and *ITGB6* expression, as it was shown in TNBC cells²¹ (online supplemental figure S8F). To examine whether ITGB6 is affecting the T-cell response in human CRC tumors, we compared ITGB6 and T-cell response marker expression in RNAseq data from the TCGA-COAD dataset, which contains data from 521 patients with CRC. *ITGB6* expression levels were widely varying between patients (figure 7B). However, by ordering the patients according to their *ITGB6* expression, we found a particularly pronounced decrease of *ITGB6* levels in the 50 patients with lowest *ITGB6* expression compared with the remaining patients (figure 7B). Therefore, we compared T-cell response marker expression of the 50 patients with lowest *ITGB6* expression (low) to the remaining 471 patients (high) (figure 7C). Similar to the observation in the RNAseq from the mouse tumors, the T-cell markers *CD8a*, *CD3d*, *CD3e*, *TRBC2*, *Il2Rb* as well as the cytotoxicity markers *GZMA*, *GZMB*, and *PRF1* were significantly upregulated in the group with low *ITGB6* expression (figure 7C). Likewise, expression of the marker for Th1 T-cell differentiation *TBX21*, the cytokine *IFN γ* , as well as the chemokine

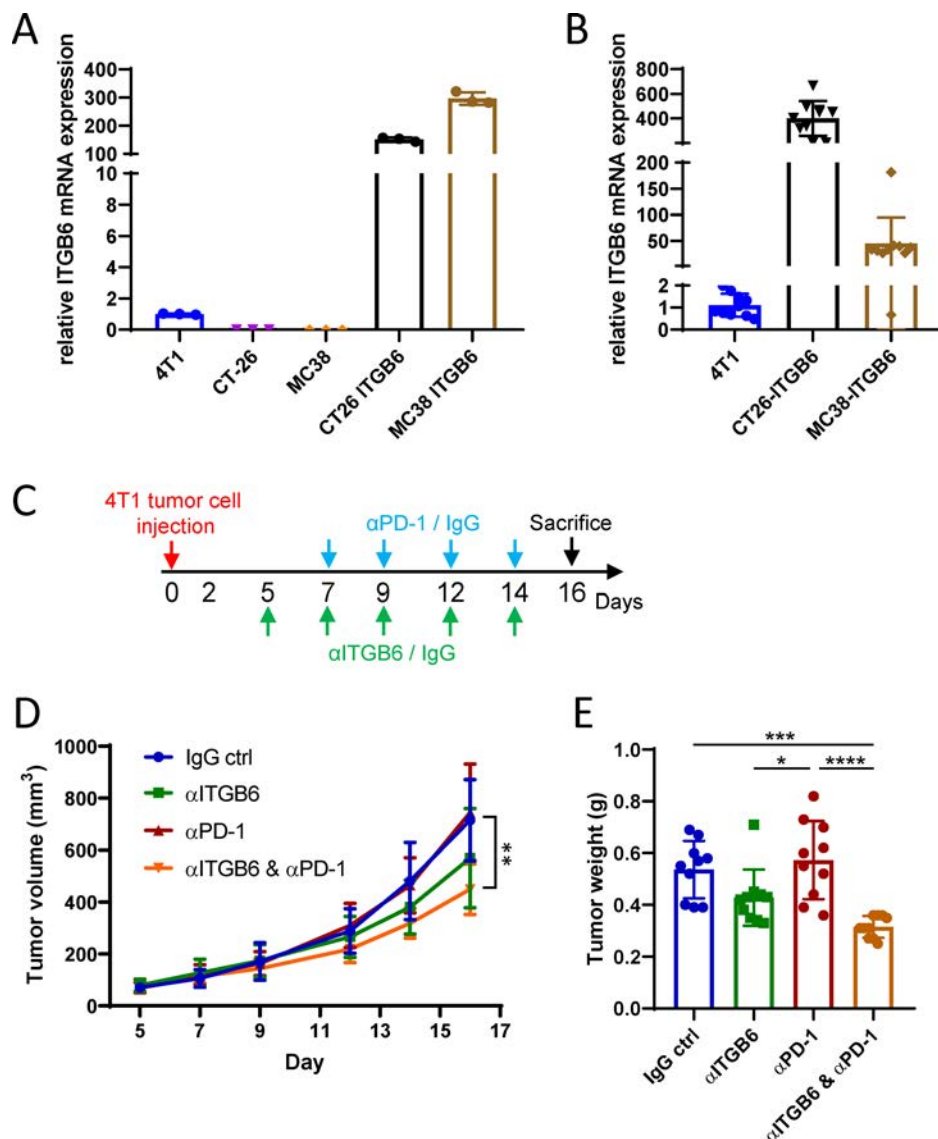


Figure 6 Integrin $\alpha v \beta 6$ blockade overcomes resistance to checkpoint blockade therapy in tumors without artificial ITGB6 overexpression. (A) RT-qPCR analysis of *Itgb6* expression in murine carcinoma cell lines. (B) RT-qPCR analysis of *Itgb6* expression in tumors grown from 4T1, CT26-ITGB6 and MC38-ITGB6 cells. (C) Experimental design of α ITGB6 (6.8G6) and α PD-1 antibody administration. (D) Tumor volume development of subcutaneous 4T1 tumors treated with α ITGB6, α PD-1, α ITGB6 and α PD-1 or IgG control. (E) Tumor weight of subcutaneous 4T1 tumors treated with α ITGB6, α PD-1, α ITGB6 and α PD-1 or IgG control. Means and SDs are shown ($n=5$ mice, 2 tumors per mouse). One-way analysis of variance (ANOVA) (E) and two way ANOVA (D) with Tukey's post-hoc test were used to calculate statistical significance. * $p<0.05$, ** $p<0.01$, *** $p<0.001$, **** $p<0.0001$.

CXCL9 were higher in that group (figure 7C). Remarkably, the patients with high *ITGB6* expression showed decreased *PD-1* expression, suggesting that ITGB6 confers resistance to α PD-1 treatment in human patients (figure 7C). Since only the samples with lowest *ITGB6* expression show an increase in T-cell response marker expression, most patients appear to have sufficient *ITGB6* expression to provoke T-cell inhibition. Therefore, the vast majority of patients would qualify for α ITGB6 treatment to overcome immune response evasion mediated by ITGB6.

DISCUSSION

Our data demonstrate that upregulation of $\alpha v \beta 6$ expression represents an effective immune evasion strategy by which tumor cells are able to escape the T-cell anticancer immune response. We showed that tumorous integrin $\alpha v \beta 6$ activates TGF- β signaling in T-cells, thereby reducing cytotoxic CD8⁺ T cell activity and infiltration. Our results very closely resemble the TGF- β -mediated inhibition of T-cells shown in previous studies, which demonstrate that activated TGF- β signaling in the tumor promotes T-cell exclusion, inhibits cytotoxic T-cell functions and provokes resistance to CBT.¹⁴⁻¹⁶ However, unlike in TNBC, where integrin $\alpha v \beta 6$ -activated TGF- β upregulates SOX4 in the tumor cells, causing resistance to T cell-mediated

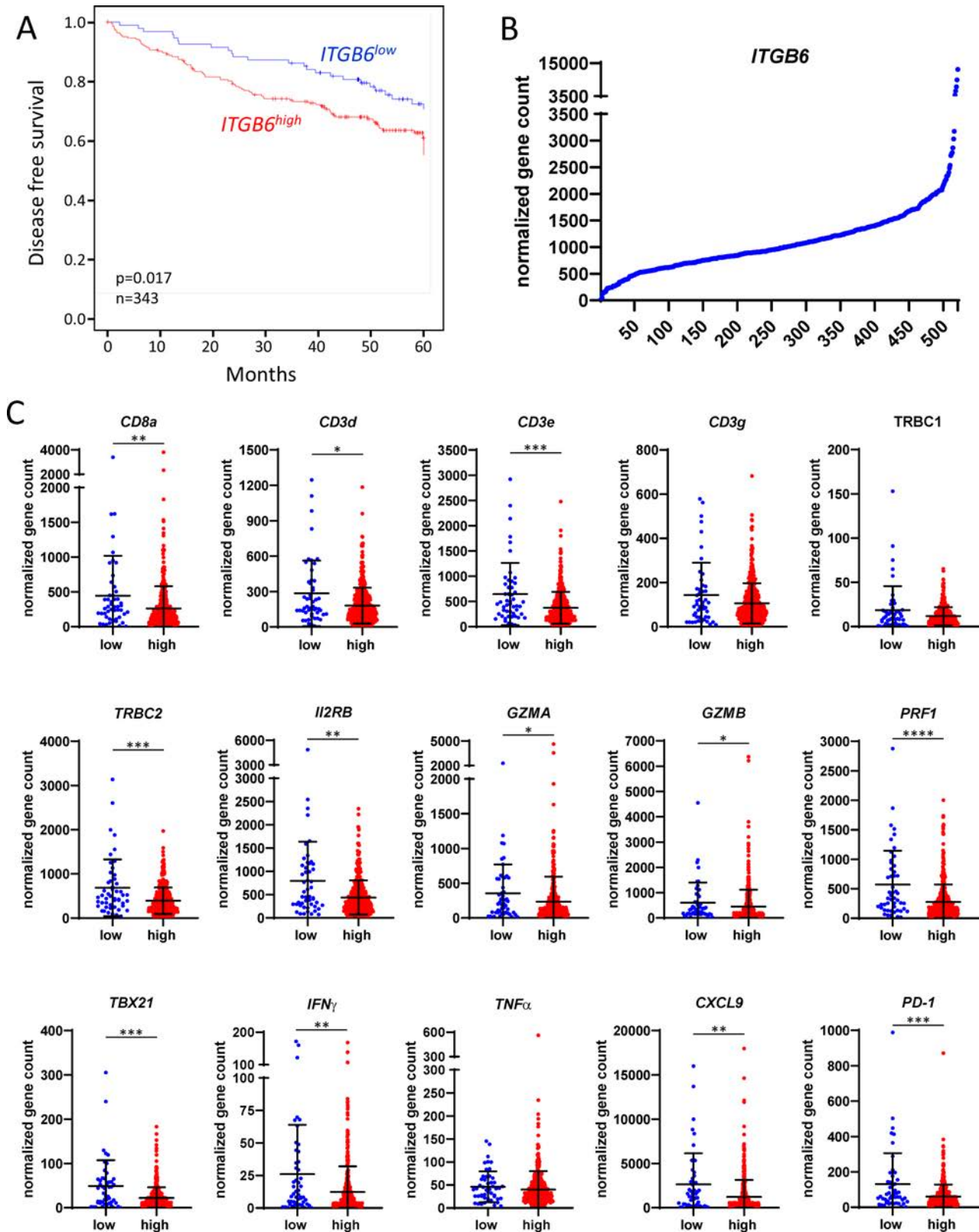


Figure 7 Integrin $\alpha v \beta 6$ inhibits T-cell immune response in the majority of patients with colorectal cancer. (A) Kaplan-Meier curves of disease free survival by *ITGB6* gene expression status. Minimum p value approach was used to obtain an optimal discrimination of the total patient group into two subgroups with different disease-free survival depending on the level of *ITGB6*. Differences in survival were compared by logrank test. *ITGB6* low: n=109, *ITGB6* high: n=234. (B) Relative *ITGB6* mRNA expression of all 521 patients in the TCGA-COAD dataset. (C) Relative mRNA expression in the 50 patients with lowest *ITGB6* expression compared with the remaining 471 patients of the TCGA-COAD dataset. Means and SDs are shown. Mann-Whitney test was used to calculate statistical significance. *P<0.05, **p<0.01, ***p<0.001, ****p<0.0001.

cytotoxicity,²¹ we did not detect an upregulation of SOX4 in our model, but identified a direct inhibiting effect of TGF- β signaling on T-cells. In any respect, integrin $\alpha\beta6$ blockade is an efficient way to prevent the tumor-promoting effects of TGF- β signaling in cancer.

Many efforts have been made to directly interfere in TGF- β signaling with the intention to provoke a therapeutic response. However, since TGF- β signaling is involved in a plethora of physiological processes, systemic TGF- β blockade often leads to harmful off-target effects, resulting in limited success of TGF- β inhibiting agents in clinical trials.^{17 18 20} Therefore, blocking this pathway at the level of TGF- β activation by inhibiting integrin $\alpha\beta6$ might be a much more promising and safe approach. Integrin $\alpha\beta6$ expression is restricted to epithelial cells and is mostly undetectable in tissue homeostasis of healthy epithelia. Apart from being upregulated during tumorigenesis of several epithelial cancers, it is only expressed during physiological events that require tissue remodeling, such as embryogenesis, endometrial cycle, wound healing, fibrosis and inflammation.^{1-3 10} This predominantly cancer-specific expression pattern presumably increases the therapeutic index of integrin $\alpha\beta6$ as a target for antibody blockade compared with the universally expressed TGF- β . Additionally, our data show that integrin $\alpha\beta6$ inhibits T-cells primarily locally in the tumor without causing systemic T-cell inhibition. Therefore, blockade of integrin $\alpha\beta6$ predominantly enhances T-cell activation in the tumor that expresses it and most likely does not cause systemic T-cell activation. In conclusion, our data demonstrate that integrin $\alpha\beta6$ represents a promising novel target for immunotherapy within the TGF- β pathway.

In previous studies, integrin $\alpha\beta6$ inhibition has already been shown to be effective in preventing tumor growth and metastasis formation in vivo.^{6 7 42} However, these studies did not discover the T-cell activating capacity of $\alpha\beta6$ inhibition and hypothesized, that other mechanisms are responsible for $\alpha\beta6$ -induced cancer progression. They found that integrin $\alpha\beta6$ activates proliferation by enhancing ERK signaling, increases protease expression and enhances epithelial to mesenchymal transition (EMT).^{6 7 42} While these mechanisms might have an additional effect in promoting an invasive phenotype and enhancing tumor growth, our data suggest that the predominant tumor growth-promoting mechanism mediated by integrin $\alpha\beta6$ is T-cell exclusion and inhibition. Therefore, the correlation of integrin $\alpha\beta6$ expression with decreased survival in cancer might not only be caused by enhanced EMT and tumor invasion, but mainly by inhibition of the T-cell immune response.

There are two major activators of latent TGF- β in vivo, integrin $\alpha\beta6$ and integrin $\alpha\beta8$. The particular importance of these two molecules for TGF- β activation was demonstrated by inhibition of $\alpha\beta6$ in $\beta8^{-/-}$ mice, which reproduces the abnormalities of TGF- $\beta1^{-/-}$ mice.⁴³ Both integrins activate TGF- β by binding the RGD peptide in the LAP, thereby releasing active TGF- β .^{11 44} Integrin

$\alpha\beta8$ has already been shown to enhance tumor growth by inhibiting infiltration of cytotoxic T-cells to the tumor. Furthermore, inhibition of $\alpha\beta8$ strongly enhances efficiency of α PD-1 treatment and causes a potent inhibition of MC38 tumor growth.⁴⁵ These data markedly resemble our findings with integrin $\alpha\beta6$ and highlight the importance of TGF- β activation and signaling for the cytotoxic T-cell response. However, although integrin $\alpha\beta8$ was also found to be expressed in different epithelial malignancies,⁴⁵ it also shows detectable protein expression levels in most healthy organs.⁴⁶ Unlike integrin $\alpha\beta6$, which is primarily expressed in epithelial tumors, inhibition of $\alpha\beta8$ therefore poses a much higher risk for harmful off-target effects. A recently published approach to combine α PD-1 treatment with an antibody that blocks both, integrin $\alpha\beta6$ and $\alpha\beta8$ ²¹ might therefore largely eliminate physiological TGF- β activation and lead to intolerable systemic side effects in patients, similar to direct TGF- β inhibition.

CBT has become the standard of care for numerous malignancies. However, while CBT has shown to be especially effective to treat highly mutated tumors with numerous neoantigens, tumors with a low mutational burden show only limited response rates.⁴⁷ In CRC, only patients that harbor microsatellite instability-high or DNA mismatch repair deficient (dMMR) tumors benefit from immunotherapy with PD-1 inhibitors and those patients represent only 3%–6% of all patients with advanced staged CRC.⁴⁸ Therefore, improvement of immunotherapy for patients with microsatellite stable (MSS) or MMR-proficient (MMR-p) tumors is urgently needed. Up to this point, clinical studies aiming to enhance the immunogenic responses by combining PD-1 inhibitors with other treatment modalities in MSS or MMR-p disease were unsuccessful.⁴⁸ Our data show that integrin $\alpha\beta6$ inhibition overcomes resistance to CBT, rendering the tumors susceptible to PD-1 inhibition. Therefore, a combination of CBT with inhibition of integrin $\alpha\beta6$ will potentially enhance an immunogenic response that might allow successful immunotherapy in MSS or MMR-p tumors. With regard to CRC, further studies will have to evaluate to what extent integrin $\alpha\beta6$ is responsible for CBT resistance of MSS or MMR-p tumors. However, since enhanced ITGB6 expression is observed in many cancers of epithelial origin, it is likely that $\alpha\beta6$ upregulation is a general mechanism of immune response evasion and that combination of CBT with $\alpha\beta6$ inhibition will increase the response rates in multiple integrin $\alpha\beta6$ expressing cancer types.

Patients with CRC show varying levels of tumorous ITGB6 expression, which negatively correlate with disease free survival. Correspondingly, we showed that the majority of CRC tumors have sufficient ITGB6 expression to provoke inhibition of the cytotoxic T-cell response. Therefore, by treating these tumors with an ITGB6 blocking antibody, the antitumor T-cell response might be activated to a similar extent as in tumors with

low ITGB6 expression and improve patient outcomes. In CRC, ITGB6 blockade therefore is a promising treatment strategy to enhance both, the T-cell response itself and the efficacy of other T-cell activating immunotherapies.

Author affiliations

¹Department of Gastroenterology and Hepatology, University Hospital Zurich, University of Zurich, Zurich, Switzerland

²Division of Molecular and Experimental Surgery, Department of Surgery, Friedrich-Alexander University Erlangen-Nuremberg, Erlangen, Germany

³Department of Physiology, University of Zurich, Zurich, Switzerland

⁴Institute of Pathology, University Hospital Erlangen, Friedrich-Alexander University Erlangen-Nuremberg, Erlangen, Germany

Acknowledgements We thank Paul Weinreb (Biogen) for the supply with antibodies. Further we thank Professor Lubor Borsig for providing us with CT26 and MC38-GFP cells. Additionally, we thank Katja Petter for excellent technical assistance.

Contributors Conceptualisation: PB, MS, MRS, GR, MSt. Formal analysis: PB, YM, EN. Investigation: PB, AM-A, EK, LH, KA, EN, CVP. Data curation: YM. Methodology: PB, SL, JFGG. Visualisation: PB, YM. Resources: AH. Writing – original draft preparation: PB. Writing – review and editing: all authors. Supervision: MS. Project administration: PB, MS. Funding acquisition: MS, MSt. Guarantor: MS

Funding The work was supported by a grant from the Stiftung Experimentelle Biomedizin to MS, a joint grant from the German Research Foundation/Swiss National Science Foundation to MS and MSt (320030E_190969), a grant from the Deutsche Forschungsgemeinschaft (DFG) – TRR 305, Subproject B08 to EN, a grant from the Swiss National Science Foundation to MS (320030_184753 and 314730_166381), a grant from the Cancer Research Center Zürich to MS and a grant from the Promedica Foundation to MS.

Competing interests None declared.

Patient consent for publication Not applicable.

Ethics approval All animal experiments were performed according to Swiss animal welfare legislation and approved by the local veterinary office (Veterinäramt des Kantons Zürich) (License numbers 239/2016 and 179/2019). Human sample collection and procedures were approved by the local ethics committee (no. 262_18 Bc; Ethikkommission der FAU, Erlangen, Germany). Informed consent was obtained from all patients before their participation in this study.

Provenance and peer review Not commissioned; externally peer reviewed.

Data availability statement RNA sequencing analysis data have been deposited in the BioProject database with accession number PRJNA798222.

Supplemental material This content has been supplied by the author(s). It has not been vetted by BMJ Publishing Group Limited (BMJ) and may not have been peer-reviewed. Any opinions or recommendations discussed are solely those of the author(s) and are not endorsed by BMJ. BMJ disclaims all liability and responsibility arising from any reliance placed on the content. Where the content includes any translated material, BMJ does not warrant the accuracy and reliability of the translations (including but not limited to local regulations, clinical guidelines, terminology, drug names and drug dosages), and is not responsible for any error and/or omissions arising from translation and adaptation or otherwise.

Open access This is an open access article distributed in accordance with the Creative Commons Attribution Non Commercial (CC BY-NC 4.0) license, which permits others to distribute, remix, adapt, build upon this work non-commercially, and license their derivative works on different terms, provided the original work is properly cited, appropriate credit is given, any changes made indicated, and the use is non-commercial. See <http://creativecommons.org/licenses/by-nc/4.0/>.

ORCID iD

Philipp Busenhardt <http://orcid.org/0000-0002-5457-7927>

REFERENCES

- 1 Bandyopadhyay A, Raghavan S. Defining the role of integrin alphavbeta6 in cancer. *Curr Drug Targets* 2009;10:645–52.
- 2 Niu J, Li Z. The roles of integrin α v β 6 in cancer. *Cancer Lett* 2017;403:128–37.

- 3 Meecham A, Marshall JF. The ITGB6 gene: its role in experimental and clinical biology. *Gene X* 2020;5:100023.
- 4 Bates RC, Bellovin DI, Brown C, *et al.* Transcriptional activation of integrin beta6 during the epithelial-mesenchymal transition defines a novel prognostic indicator of aggressive colon carcinoma. *J Clin Invest* 2005;115:339–47.
- 5 Bengs S, Becker E, Busenhardt P, *et al.* β_6 -integrin serves as a novel serum tumor marker for colorectal carcinoma. *Int J Cancer* 2019;145:678–85.
- 6 Moore KM, Thomas GJ, Duffy SW, *et al.* Therapeutic targeting of integrin α v β 6 in breast cancer. *J National Cancer Institute* 2014;106.
- 7 Reader CS, Vallath S, Steele CW, *et al.* The integrin α v β 6 drives pancreatic cancer through diverse mechanisms and represents an effective target for therapy. *J Pathol* 2019;249:332–42.
- 8 Elayadi AN, Samli KN, Prudkin L, *et al.* A peptide selected by biopanning identifies the integrin alphavbeta6 as a prognostic biomarker for nonsmall cell lung cancer. *Cancer Res* 2007;67:5889–95.
- 9 Hazelbag S, Kenter GG, Gorter A, *et al.* Overexpression of the alpha v beta 6 integrin in cervical squamous cell carcinoma is a prognostic factor for decreased survival. *J Pathol* 2007;212:316–24.
- 10 Koivisto L, Bi J, Häkkinen L, *et al.* Integrin α v β 6: structure, function and role in health and disease. *Int J Biochem Cell Biol* 2018;99:186–96.
- 11 Brown NF, Marshall JF. Integrin-Mediated TGF β activation modulates the tumour microenvironment. *Cancers* 2019;11:1221.
- 12 Battle E, Massagué J. Transforming growth factor- β signaling in immunity and cancer. *Immunity* 2019;50:924–40.
- 13 Dahmani A, Delisle J-S. TGF- β in T cell biology: implications for cancer immunotherapy. *Cancers* 2018;10:1. doi:10.3390/cancers10060194
- 14 Tauriello DVF, Palomo-Ponce S, Stork D, *et al.* TGF β drives immune evasion in genetically reconstituted colon cancer metastasis. *Nature* 2018;554:538–43.
- 15 Mariathasan S, Turley SJ, Nickles D, *et al.* TGF β attenuates tumour response to PD-L1 blockade by contributing to exclusion of T cells. *Nature* 2018;554:544–8.
- 16 Martin CJ, Datta A, Littlefield C, *et al.* Selective inhibition of TGF β 1 activation overcomes primary resistance to checkpoint blockade therapy by altering tumor immune landscape. *Sci Transl Med* 2020;12.
- 17 Akhurst RJ. Targeting TGF- β signaling for therapeutic gain. *Cold Spring Harb Perspect Biol* 2017;9. doi:10.1101/cshperspect.a022301
- 18 Connolly EC, Freimuth J, Akhurst RJ. Complexities of TGF- β targeted cancer therapy. *Int J Biol Sci* 2012;8:964–78.
- 19 Anderton MJ, Mellor HR, Bell A, *et al.* Induction of heart valve lesions by small-molecule ALK5 inhibitors. *Toxicol Pathol* 2011;39:916–24.
- 20 Huynh L, Hipolito C, ten Dijke P. A perspective on the development of TGF- β inhibitors for cancer treatment. *Biomolecules* 2019;9:743.
- 21 Bagati A, Kumar S, Jiang P, *et al.* Integrin α v β 6-TGF β -SOX4 pathway drives immune evasion in triple-negative breast cancer. *Cancer Cell* 2021;39:54–67.
- 22 Mohammed J, Beura LK, Bobr A, *et al.* Stromal cells control the epithelial residence of DCs and memory T cells by regulated activation of TGF- β . *Nat Immunol* 2016;17:414–21.
- 23 Campeau E, Ruhl VE, Rodier F, *et al.* A versatile viral system for expression and depletion of proteins in mammalian cells. *PLoS One* 2009;4:e6529.
- 24 Weinreb PH, Simon KJ, Rayhorn P, *et al.* Function-blocking integrin alphavbeta6 monoclonal antibodies: distinct ligand-mimetic and nonligand-mimetic classes. *J Biol Chem* 2004;279:17875–87.
- 25 Spalinger MR, Kasper S, Gottier C, *et al.* NLRP3 tyrosine phosphorylation is controlled by protein tyrosine phosphatase PTPN22. *J Clin Invest* 2016;126:1783–800.
- 26 Spalinger MR, Schwarzfischer M, Hering L, *et al.* Loss of PTPN22 abrogates the beneficial effect of cohousing-mediated fecal microbiota transfer in murine colitis. *Mucosal Immunol* 2019;12:1336–47.
- 27 Love MI, Huber W, Anders S. Moderated estimation of fold change and dispersion for RNA-seq data with DESeq2. *Genome Biol* 2014;15:550.
- 28 Huang DW, Sherman BT, Lempicki RA. Systematic and integrative analysis of large gene lists using DAVID bioinformatics resources. *Nat Protoc* 2009;4:44–57.
- 29 Huang DW, Sherman BT, Lempicki RA. Bioinformatics enrichment tools: paths toward the comprehensive functional analysis of large gene Lists. *Nucleic Acids Res* 2009;37:1–13.
- 30 Finotello F, Mayer C, Plattner C, *et al.* Molecular and pharmacological modulators of the tumor immune contexture revealed by deconvolution of RNA-seq data. *Genome Med* 2019;11:34.



- 31 Robinson MD, McCarthy DJ, Smyth GK. edgeR: a Bioconductor package for differential expression analysis of digital gene expression data. *Bioinformatics* 2010;26:139–40.
- 32 McCarthy DJ, Chen Y, Smyth GK. Differential expression analysis of multifactor RNA-Seq experiments with respect to biological variation. *Nucleic Acids Res* 2012;40:4288–97.
- 33 Agrez M, Chen A, Cone RI, et al. The alpha v beta 6 integrin promotes proliferation of colon carcinoma cells through a unique region of the beta 6 cytoplasmic domain. *J Cell Biol* 1994;127:547–56.
- 34 Dixit RB, Chen A, Chen J, et al. Identification of a sequence within the integrin beta6 subunit cytoplasmic domain that is required to support the specific effect of alphavbeta6 on proliferation in three-dimensional culture. *J Biol Chem* 1996;271:25976–80.
- 35 Li X, Yang Y, Hu Y, et al. Alphavbeta6-Fyn signaling promotes oral cancer progression. *J Biol Chem* 2003;278:41646–53.
- 36 Tokunaga R, Zhang W, Naseem M, et al. CXCL9, CXCL10, CXCL11/CXCR3 axis for immune activation - A target for novel cancer therapy. *Cancer Treat Rev* 2018;63:40–7.
- 37 Calon A, Espinet E, Palomo-Ponce S, et al. Dependency of colorectal cancer on a TGF- β -driven program in stromal cells for metastasis initiation. *Cancer Cell* 2012;22:571–84.
- 38 Calon A, Lonardo E, Berenguer-Llergo A, et al. Stromal gene expression defines poor-prognosis subtypes in colorectal cancer. *Nat Genet* 2015;47:320–9.
- 39 Gorelik L, Flavell RA. Abrogation of TGFbeta signaling in T cells leads to spontaneous T cell differentiation and autoimmune disease. *Immunity* 2000;12:171–81.
- 40 Vodenkova S, Buchler T, Cervena K, et al. 5-fluorouracil and other fluoropyrimidines in colorectal cancer: past, present and future. *Pharmacol Ther* 2020;206:107447.
- 41 Wu Y, Deng Z, Wang H, et al. Repeated cycles of 5-fluorouracil chemotherapy impaired anti-tumor functions of cytotoxic T cells in a CT26 tumor-bearing mouse model. *BMC Immunol* 2016;17:29.
- 42 Eberlein C, Kendrew J, McDaid K, et al. A human monoclonal antibody 264RAD targeting $\alpha v \beta 6$ integrin reduces tumour growth and metastasis, and modulates key biomarkers in vivo. *Oncogene* 2013;32:4406–16.
- 43 Aluwihare P, Mu Z, Zhao Z, et al. Mice that lack activity of alphavbeta6- and alphavbeta8-integrins reproduce the abnormalities of Tgfb1- and Tgfb3-null mice. *J Cell Sci* 2009;122:227–32.
- 44 Shi M, Zhu J, Wang R, et al. Latent TGF- β structure and activation. *Nature* 2011;474:343–9.
- 45 Takasaka N, Seed RI, Cormier A, et al. Integrin $\alpha v \beta 8$ -expressing tumor cells evade host immunity by regulating TGF- β activation in immune cells. *JCI Insight* 2018;3 doi:10.1172/jci.insight.122591
- 46 McCarty JH. $\alpha v \beta 8$ integrin adhesion and signaling pathways in development, physiology and disease. *J Cell Sci* 2020;133 doi:10.1242/jcs.239434
- 47 Robert C. A decade of immune-checkpoint inhibitors in cancer therapy. *Nat Commun* 2020;11:3801.
- 48 Golshani G, Zhang Y. Advances in immunotherapy for colorectal cancer: a review. *Therap Adv Gastroenterol* 2020;13:1756284820917527.

Supplemental material

SUPPLEMENTAL METHODS

Cloning

Amplified ITGB6 and pLenti CMV GFP Blast vector were digested with BamHI (NEB; R3136) and Sall (NEB; R3138) restriction enzymes and ligated with Quick ligation kit (NEB; M2200). Control vector was constructed by ligating a short non-coding oligonucleotide instead of the amplified ITGB6 gene.

Primers containing BamHI and Sall restriction sites for PCR amplification of ITGB6:

TAAGGATCCGCCACCATGGGGATTGAGCTGGTCTG

TAAGTCGACAGCGGCCTACCCATCTGAGGAAAGGCC

Lentivirus production and viral transduction

In a T75 cell culture flask, HEK 293T cells were transfected with 9 µg ITGB6 expression vector, 4 µg pMD2.G (Addgene plasmid # 12259) and 7 µg pCMV-dR8.91 (Addgene vector database # 2221) using Lipofectamine 3000 reagent (Thermo Fisher Scientific) according to the manufacturers protocol for lentiviral production. After 6h, transfection medium was removed and 10 ml fresh growth medium added. Supernatant containing the viral particles was harvested 24h and 48h later, filtered with 0.45 µm pore size, and frozen at -80°C.

CT26 and MC38-GFP cells (donated by Prof. Lubor Borsig, Institute of Physiology, University of Zurich, Zurich) were seeded at ~60% confluency and transduced by adding viral supernatant together with 8 µg/ml Polybrene (Merck; H9268). After 24h viral medium was removed and fresh growth medium added. 48h after initiation of transduction blasticidine selection was started by adding fresh medium containing 5 µg/ml blasticidine (Merck; 15205) and continued until untransduced control cells were completely dead.

Proliferation assay

In 96-well plates, MC38-ITGB6 and MC38-Ctrl as well as CT26-ITGB6 and CT26-Ctrl cells were seeded at 125 cells per well. After 24h (d0) or 96h (d3), cell number was defined using CellTiter-Glo® Luminescent Cell Viability Assay (Promega G7571) according to manufacturer's instructions and measured using BioTek Synergy 2 Microplate Reader.

Western Blot

Cells were lysed in RIPA cell lysis buffer (25 mM Tris-HCl pH 7.6, 150 mM sodium chloride, 1% NP-40, 1% sodium deoxycholate, 0.1% SDS) with cOmplete™ Mini Protease Inhibitor Cocktail (Merck; 11836153001). Protein extracts (20 µg) were run on 10% polyacrylamide gels, transferred to nitrocellulose membranes and visualized by immunoblotting with ITGB6 antibody (R&D Systems; MAB2389) and anti-mouse IgG-HRP (Santa Cruz; sc-2005).

Co-Immunoprecipitation

Cells were lysed in IP lysis buffer (20mM Tris-HCL pH 7.5, 150mM sodium chloride, 1% IGEPAL, 5mM magnesium chloride) with cOmplete™ Mini Protease Inhibitor Cocktail (Roche; 04693132001) and sonicated. Protein extracts (1 mg) were incubated overnight with protein A beads fast flow (Cytiva; 17528001) pre-coated with 2 µg ITGB6 antibody (R&D Systems; AF4155) at 4°C. Beads were washed with IP Wash buffer (20mM Tris-HCL pH 7.5, 150mM sodium chloride, 0,1% IGEPAL, 5mM magnesium chloride) and taken up in Laemmli buffer. Eluted samples were applied to 12,5% polyacrylamide gels transferred to nitrocellulose membranes and visualized by immunoblotting with ITGB6 antibody (R&D Systems; AF4155), ITGA antibody (abcam, ab179475), anti-rabbit IgG-HRP (Dako; P0448) and anti-sheep IgG-HRP (R&D Systems; HAF016).

Tumor cell injections

CT26-ITGB6 and CT26-Ctrl tumor cells were suspended in DMEM high glucose cell culture medium mixed 1:1 with matrigel (Corning 354263) and 60'000 cells were injected into the cecum wall (orthotopic model) or 100'000 cells were injected subcutaneously into the flanks (heterotopic model). MC38-ITGB6 and MC38-Ctrl tumor cells were suspended in DMEM high glucose cell culture medium mixed 1:1 with matrigel and 300'000 cells were injected subcutaneously into the flanks of the mice. 4T1 breast cancer cells (ATCC® CRL-2539™) were suspended in RPMI 1640 cell culture medium mixed 1:1 with matrigel and 100'000 cells subcutaneously injected subcutaneously into the flanks of the mice.

Histology

For histological studies, mouse tumors were fixed in 4% formalin, dehydrated by a graded series of ethanol (70 to 100%) and embedded in paraffin wax. 5 µm sections were cut using a rotary microtome

(Zeiss Hymam M 15). To further process the samples, the tissue sections were deparaffinized with Histo Clear (Chemie Brunschwig/National Diagnostics, HS-200) and rehydrated using a graded series of ethanol (100% to 70%).

For mouse IHC stainings, the rehydrated samples were heated (98 C°) for 30 min in antigen retrieval solution (Dako; S169984; Target Retrieval Solution; pH: 6.0). Endogenous peroxidases were blocked for 15 minutes with 0.9% H₂O₂ in PBS and unspecific antibody binding blocked by incubation with 2.5% horse serum for 1 hour. Primary antibodies CD8 (Cell Signaling; CD8α (D4W2Z) XP® Rabbit mAb #9894), CD4 (Cell Signaling; CD4 (D7D2Z) Rabbit mAb #25229), CD3 (Abcam; Anti-CD3 ab5690), Ki67 (Fisher Scientific; 12693697, RM-9106-S), pSmad2 (Cell Signaling; Phospho-Smad2 (Ser465/467) (138D4) #3108), pSmad3 (Abcam; Anti-Smad3 (phospho S423 + S425) [EP823Y] ab52903), CALD1 (Merck; Anti-CALD1 HPA008066), IGFBP7 (Merck; Anti-IGFBP7 HPA002196), SOX4 (Abcam; Anti-SOX4 ab86809) were incubated at 4 °C overnight. On the next day, the slides were incubated for 1 hour with the secondary antibody (Vector Laboratories; VC-MP-7401-L050 ImmPRESS™ anti-Rabbit IgG HRP; 1 drop) at room temperature followed by 1 minute DAB staining (Vector Laboratories; VC-SK-4105-L120; DAB ImmPACT™ DAB Peroxidase Substrate brown). Lastly, the sections were counterstained for 10 seconds with hematoxylin (Schleicher&Schuell; 10311651), dehydrated and mounted. The processed samples were examined under a light microscope (Zeiss Imager. Z2) and images were taken at 10X magnification. Quantification of positive cells was performed using Image J Software, 1.52a.

For IF stainings, the rehydrated samples were heated (98 C°) for 30 min in antigen retrieval solution (Dako; S236784; Target Retrieval Solution; pH: 9.0). Unspecific antibody binding was blocked by incubation with 2.5% horse serum for 1 hour. Primary antibodies CD8 (Thermo Fisher Scientific; CD8a (4SM15) 14-0808-82) and pSmad3 (Abcam; Anti-Smad3 (phospho S423 + S425) [EP823Y] ab52903), were incubated at 4 °C overnight. On the next day, the slides were incubated for 1 hour with the secondary antibodies (Thermo Fisher Scientific; Goat anti-rat Alexa Fluor 594, A11007) (Thermo Fisher Scientific; Goat anti-rabbit Alexa Fluor 647, A21244) at room temperature, washed and mounted. The processed samples were examined under a light microscope (Zeiss Imager. Z2) and images were taken at 20X or 40X magnification.

For human IHC stainings, archived formalin-fixed, paraffin-embedded human colorectal carcinoma tissue was cut in 4-µm sections using a rotary microtome (Zeiss HM 355S). The sections were

deparaffinised at 60°C overnight and rehydrated using a graded series of ethanol (100% to 70%). The rehydrated samples were heated in antigen retrieval solution (Dako; S2369; Target Retrieval Solution; pH: 6.0) in a water bath for 20 minutes at 95°C. Endogenous peroxidases were blocked by 7,5% H₂O₂ in demineralized water for 10 minutes and endogenous biotin was blocked with an Avidin/Biotin Blocking kit (Biozol; # SP-2001). Subsequently, the sections were incubated with primary Sox4 antibody (Invitrogen; PA5-41442) diluted 1:70 in 2,5% normal horse serum for 60 minutes at room temperature. The sections were incubated with Biotinylated Antibody for 30 minutes followed by the ABC reagent for 30 minutes at room temperature (Horse anti-Rabbit IgG Vectastain Elite ABC-Kit; Biozol #PK-7200). The immunodetection was performed with the NovaRed substrate kit (Vector; #SK-4800) for 4 minutes at room temperature. The sections were counterstained with Haematoxylin (Vector; H-3401), dehydrated and mounted in Vectamount Permanent Mounting Medium (Vector; # H-5000). The processed samples were examined under a light microscope (Leica CTR 6000) and images were taken at 20X magnification.

RT-qPCR analysis of mouse tumor

Tumor tissues (0.5 cm) were homogenized using gentleMACS (Miltenyi Biotec, Bergisch Gladbach, Germany) and RNA isolated using the Maxwell RSC simplyRNA Tissue kit (Promega, Madison, WI, USA) according to the manufacturer's instructions. RNA concentration was measured using absorbance at 260 and 280 nm. Complementary DNA (cDNA) was synthesized using the high-capacity cDNA reverse transcription kit (Thermo Fisher Scientific, Waltham, MA USA) according to the manufacturer's instructions. RT-PCR was performed using FAST qPCR Master Mix and pre-designed Taqman assays (Thermo Fisher Scientific, USA) on a QuantStudio 6 system using the QuantStudio software (Thermo Fisher Scientific, USA). Mouse GAPDH or β -actin were used as endogenous controls. Relative expression levels were calculated according to the $\Delta\Delta$ CT method and samples were measured in triplicates.

RT-qPCR analysis of human tumor specimen

Total RNA was isolated using a fully automated extraction method from FFPE tissue sections (Tissue Preparation System with VERSANT Tissue Preparation Reagents, Siemens Healthcare Diagnostics, Tarrytown, NY) as described previously^{1,2}. *ITGB6* was detected using a TaqMan™ Gene Expression Assay (Thermo Fisher Scientific #4351368) according to the manufacturers instructions. Additional

controls for the detection of the housekeeping gene (RPL37A) and absence of DNA contamination (PAEP) were performed as previously described^{1,2}. The SuperScript III Platinum One-Step Quantitative RT-PCR-System with ROX (LifeTechnologies) was used as recommended by the manufacturer except for a prolonged reverse transcription time of 30 min at 50°C. A reaction (10 µl total volume) consisted of 0.2 µl RT/Taq-mix, 50 nM ROX Reference Dye (Life Technologies), 10 ng total RNA, 500 nM forward/reverse primer each and 250 nM probe. The reactions were assayed in using a Mx3005P qPCR system (Agilent) together with the Versant kPCR software (Siemens Healthcare Diagnostics). For quantification of RNA samples the absence of residual DNA was analyzed by DNA-specific primers for the *progesterone-associated endometrial protein (PAEP)* gene and was in all cases negative. On each plate a commercial qPCR human reference total RNA (qRef, Agilent) was used as a positive control and a non-template control (NTC) as negative control. The fluorescence threshold (ROX dRn) was set to 0.02 for all samples. All samples were normalized using RPL37A (mean of triplicates) as a reference gene. Subsequently, the $\Delta\Delta\text{CT}$ method was used for calculation of the respective fold changes for each target gene.

The sequences of primers and probes were as follows:

RPL37A forward: 5'-TGTGGTTCCTGCATGAAGACA-3', reverse: 5'-GTGACAGCGGAAGTGGTATTGTAC-3', probe: 5'-Fam-TGGCTGGCGGTGCCTGGA-BHQ1-3';
PAEP forward: 5'-CACAGAATGGACGCCATGAC-3', reverse: 5'-AAACCAGAGAGGCCACCCTAA-3',
probe: 5'-Fam-AAGCCCTCAGCCCTGCTCTCCATC-BHQ1-3'.

SUPPLEMENTAL DATA

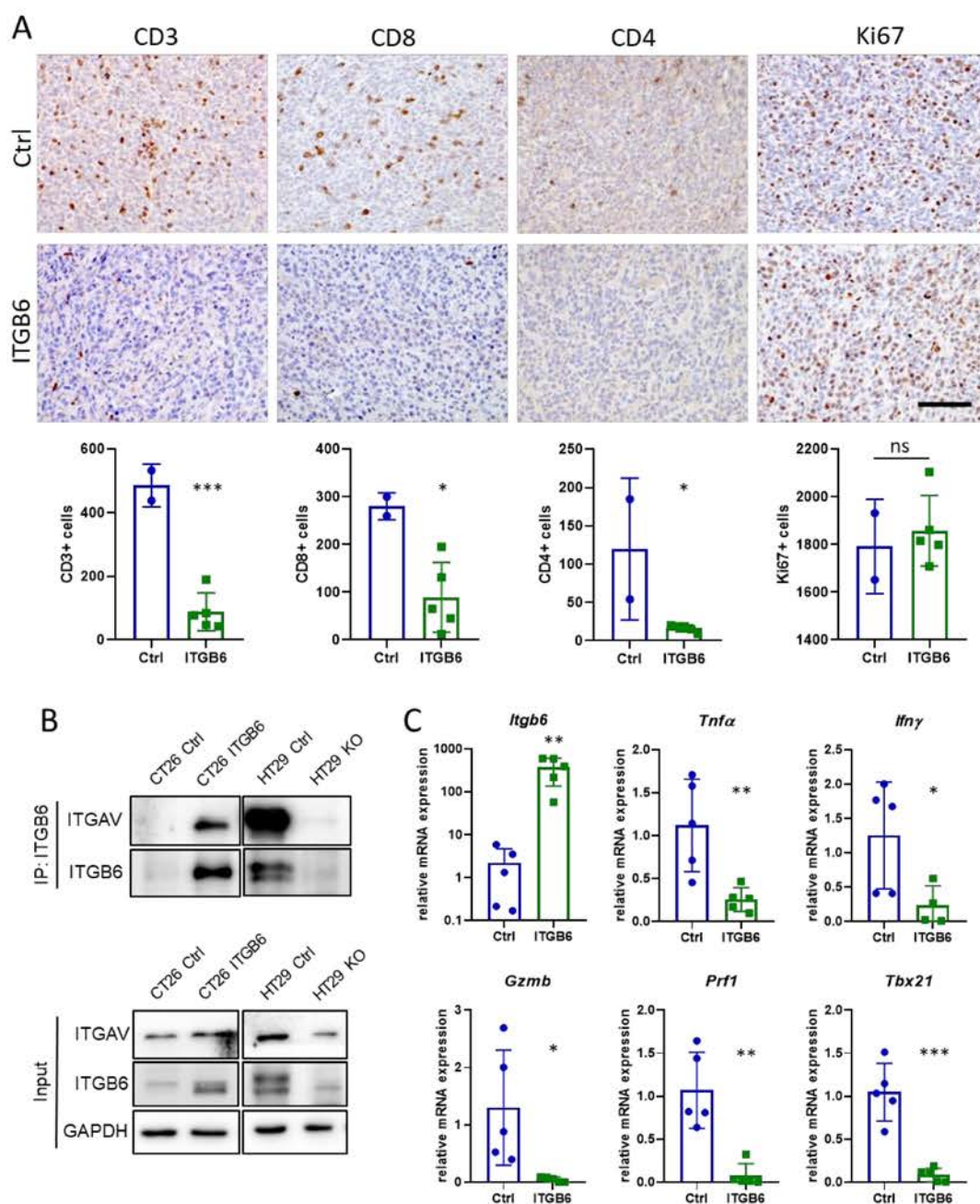


Fig. S1. (A) IHC stainings of CD3, CD4, CD8 and Ki67 in CT26-ITGB6 and CT26-Ctrl cecum tumors. Representative images of IHC stainings (top) and quantification of the number of stained cells (bottom) (n=2 (Ctrl), 5 (ITGB6)). (B) Co-immunoprecipitation of ITGAV and ITGB6. Immunoprecipitation with ITGB6 antibody (top) and expression of the input cells (bottom) HT29 knockout (KO) cells as technical control. (C) RT-qPCR analysis of anti-tumor immune mediators in tumor tissue of CT26-ITGB6 and CT26-Ctrl cecum tumors (n=5). Scale bar = 100 μ m. Means and SDs are shown. Unpaired two-tailed t-tests were used to calculate statistical significance. ns = not significant ($p \geq 0.05$), * $p < 0.05$, ** $p < 0.01$, *** $p < 0.001$, **** $p < 0.0001$.

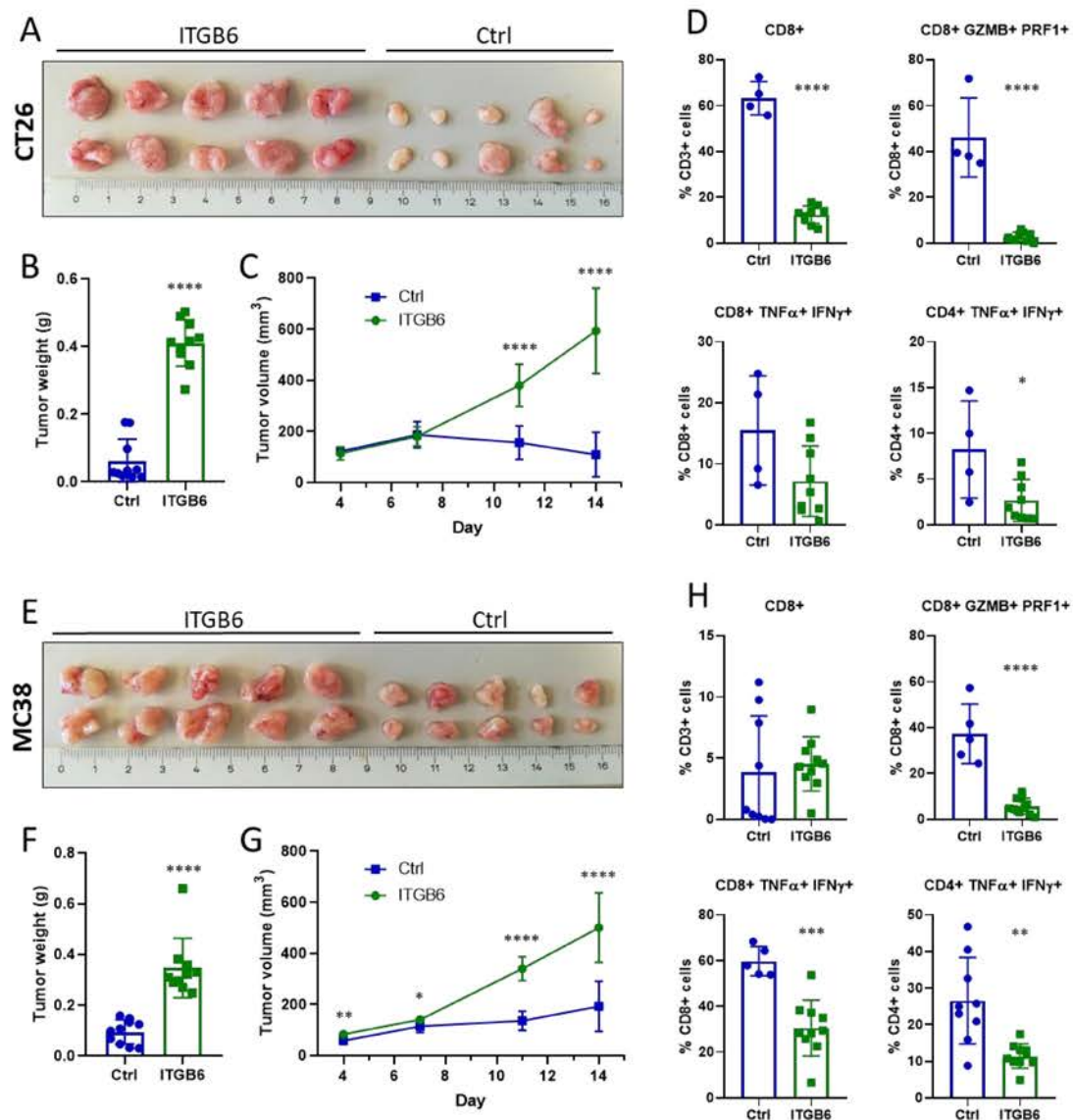


Fig. S2. (A) Subcutaneous CT26-ITGB6 and CT26-Ctrl tumors at day 14 after injection into Balb/c mice. (B) Weight of CT26-ITGB6 and CT26-Ctrl tumors at day 14 after injection. (C) Tumor volume development of CT26-ITGB6 and CT26-Ctrl tumors. (D) Flow cytometry analysis of T-cells isolated from CT26-ITGB6 and CT26-Ctrl tumors. (E) Subcutaneous MC38-ITGB6 and MC38-Ctrl tumors at day 14 after injection into C57BL/6 mice. (F) Weight of MC38-ITGB6 and MC38-Ctrl tumors at day 14 after injection. (G) Tumor volume development of MC38-ITGB6 and MC38-Ctrl tumors. (H) Flow cytometry analysis of T-cells isolated from MC38-ITGB6 and MC38-Ctrl tumors. Means and SDs are shown (n=5 mice, 2 tumors per mouse). Unpaired two-tailed t-test (B, D, F, H) and two-way ANOVA with Tukey's post-hoc test (C and G) were used to calculate statistical significance. *p < 0.05, **p < 0.01, ***p < 0.001, ****p < 0.0001.

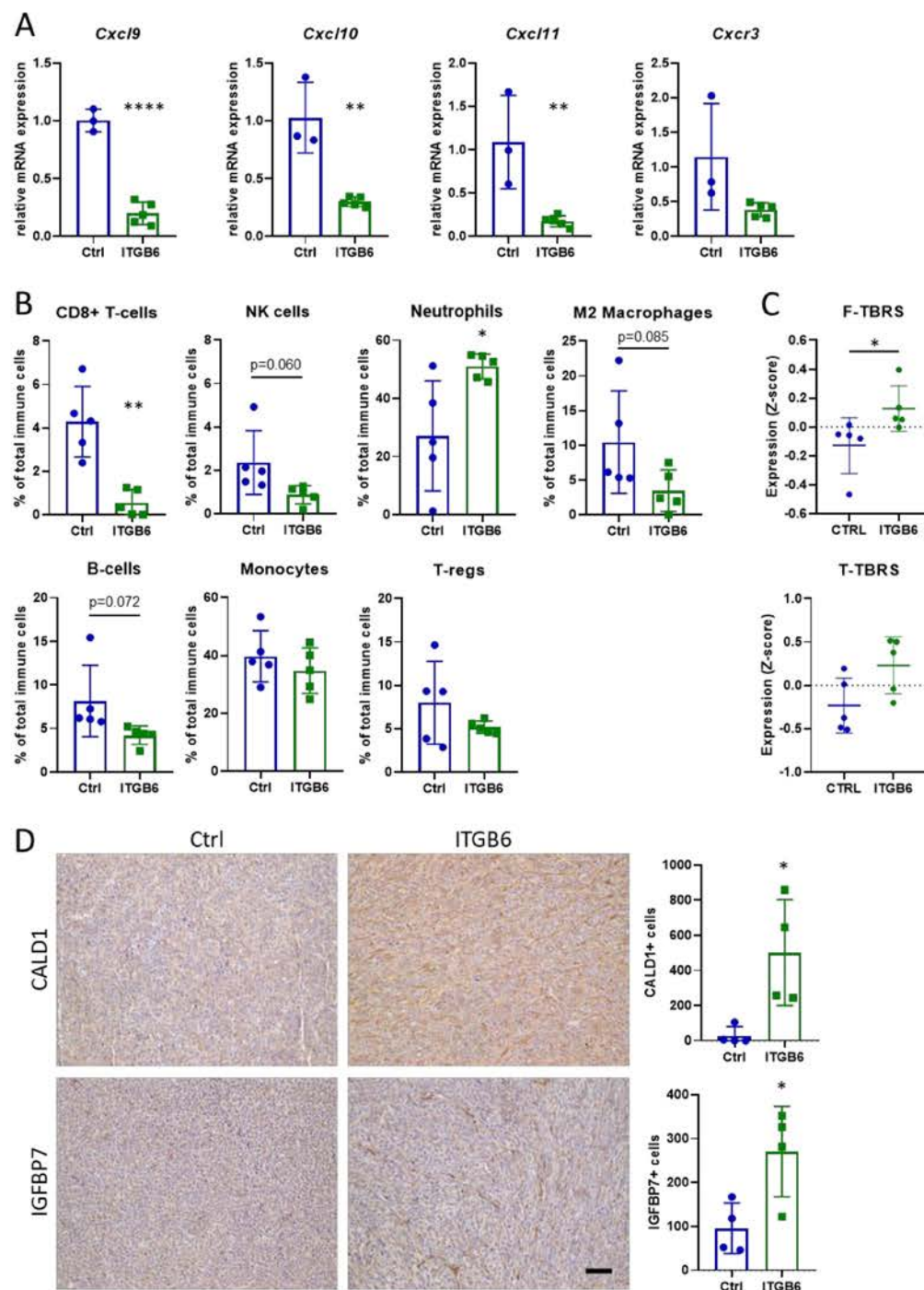


Fig. S3. (A) RT-qPCR analysis of subcutaneous CT26-ITGB6 and CT26-Ctrl tumors. (B) Deconvolution of immune cell type proportions from the bulk tissue RNA-seq data of MC38-ITGB6 and MC38-Ctrl tumors based on a reference expression signature panel. (C) Expression levels of TBRS in fibroblasts (F-TBRS) and T-cells (T-TBRS) in MC38-ITGB6 and MC38-Ctrl tumors (D) IHC stainings of CALD1 and IGFBP7 in subcutaneous CT26-ITGB6 and CT26-Ctrl tumors. Representative images of IHC stainings (left) and quantification of the number of stained cells (right). Scale bar = 100 μ m. Means and SDs are shown (n=5). Unpaired two-tailed t-tests were used to calculate statistical significance. * $p < 0.05$, ** $p < 0.01$, *** $p < 0.001$, **** $p < 0.0001$.

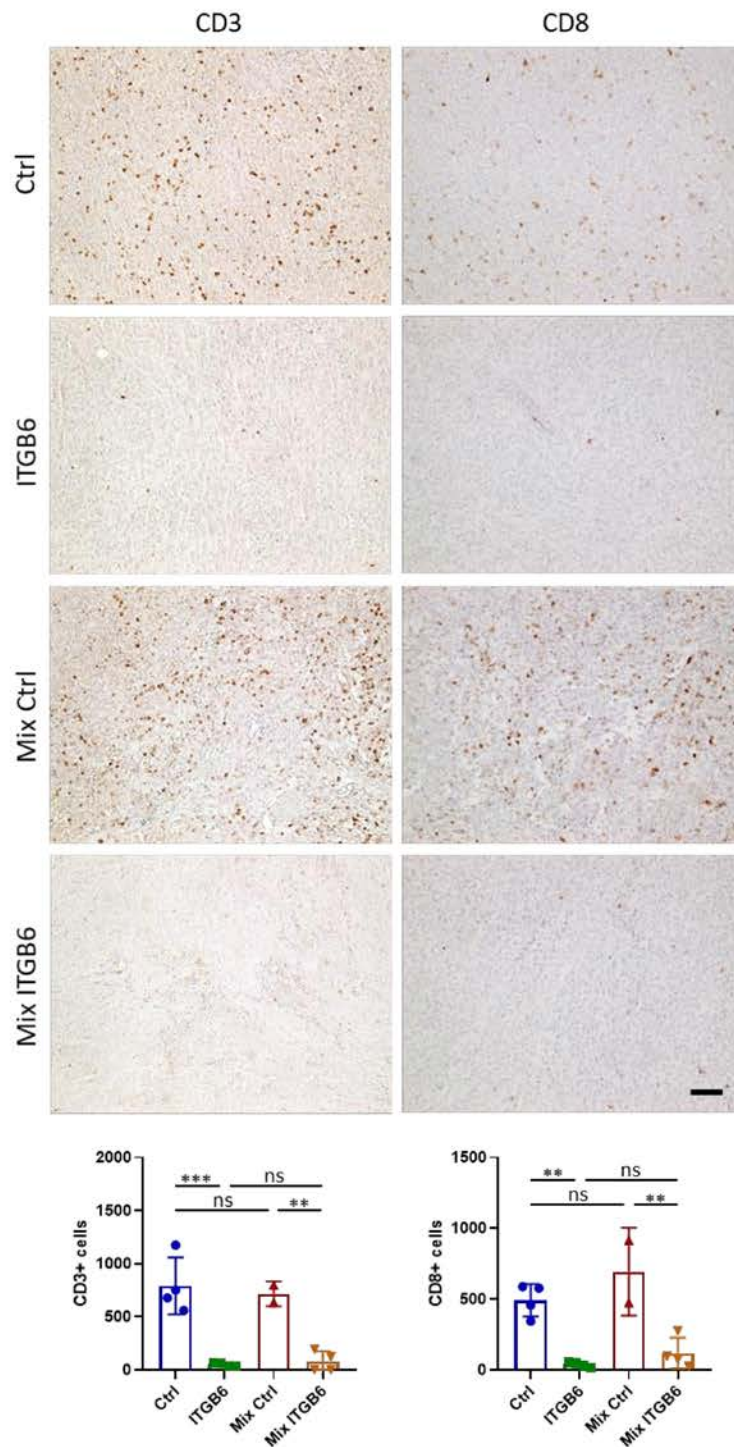


Fig. S4. IHC stainings of CD3 and CD8 in subcutaneous CT26-Ctrl tumors or CT26-ITGB6 tumors injected in both flanks or CT26-Ctrl tumors in one flank and CT26-ITGB6 tumors in the other flank of the mice (Mix). Representative images of IHC stainings (top) and quantification of the number of stained cells (bottom). Scale bar = 100 μ m. Means and SDs are shown (n=2-5). One-way ANOVA with Tukey's post-hoc test was used to calculate statistical significance. *p < 0.05, **p < 0.01, ***p < 0.001, ****p < 0.0001.

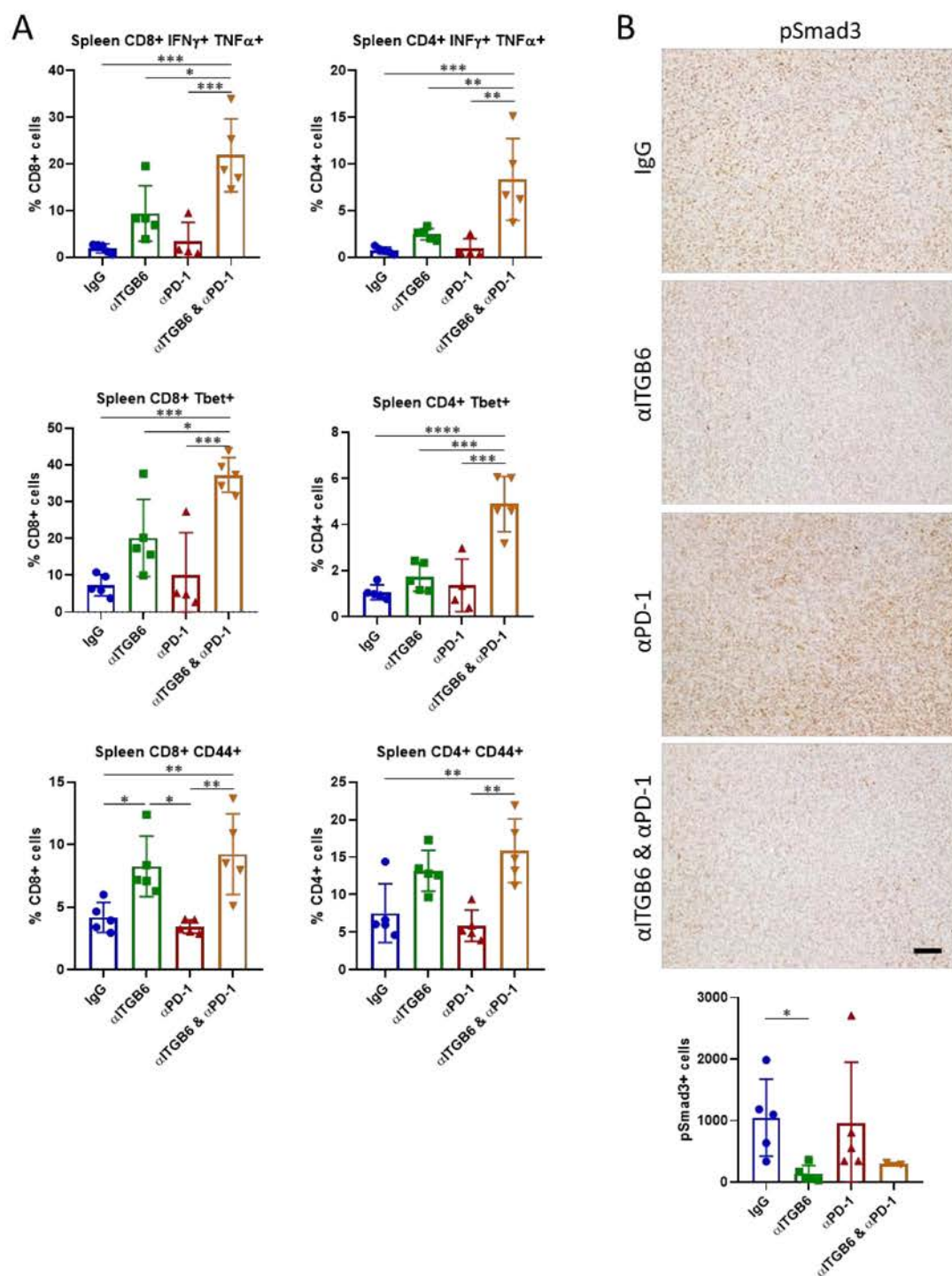


Fig. S5. (A) Flow cytometry analysis of splenic CD8+ and CD4+ T-cells in mice bearing CT26-ITGB6 tumors treated with α ITGB6 (6.8G6), α PD-1, α ITGB6 (6.8G6) & α PD-1 or IgG control antibody. (B) IHC staining of pSmad3 in subcutaneous CT26-ITGB6 tumors treated with α ITGB6 (6.8G6), α PD-1, α ITGB6 (6.8G6) & α PD-1 or IgG control antibody. Representative images of IHC staining (top) and quantification of the number of stained cells (bottom). Scale bar = 100 μ m. Means and SDs are shown (n=5 mice). One-way ANOVA with Tukey's post-hoc test (A) and unpaired two-tailed t-test (B) was used to calculate statistical significance. *p < 0.05, **p < 0.01, ***p < 0.001, ****p < 0.0001.

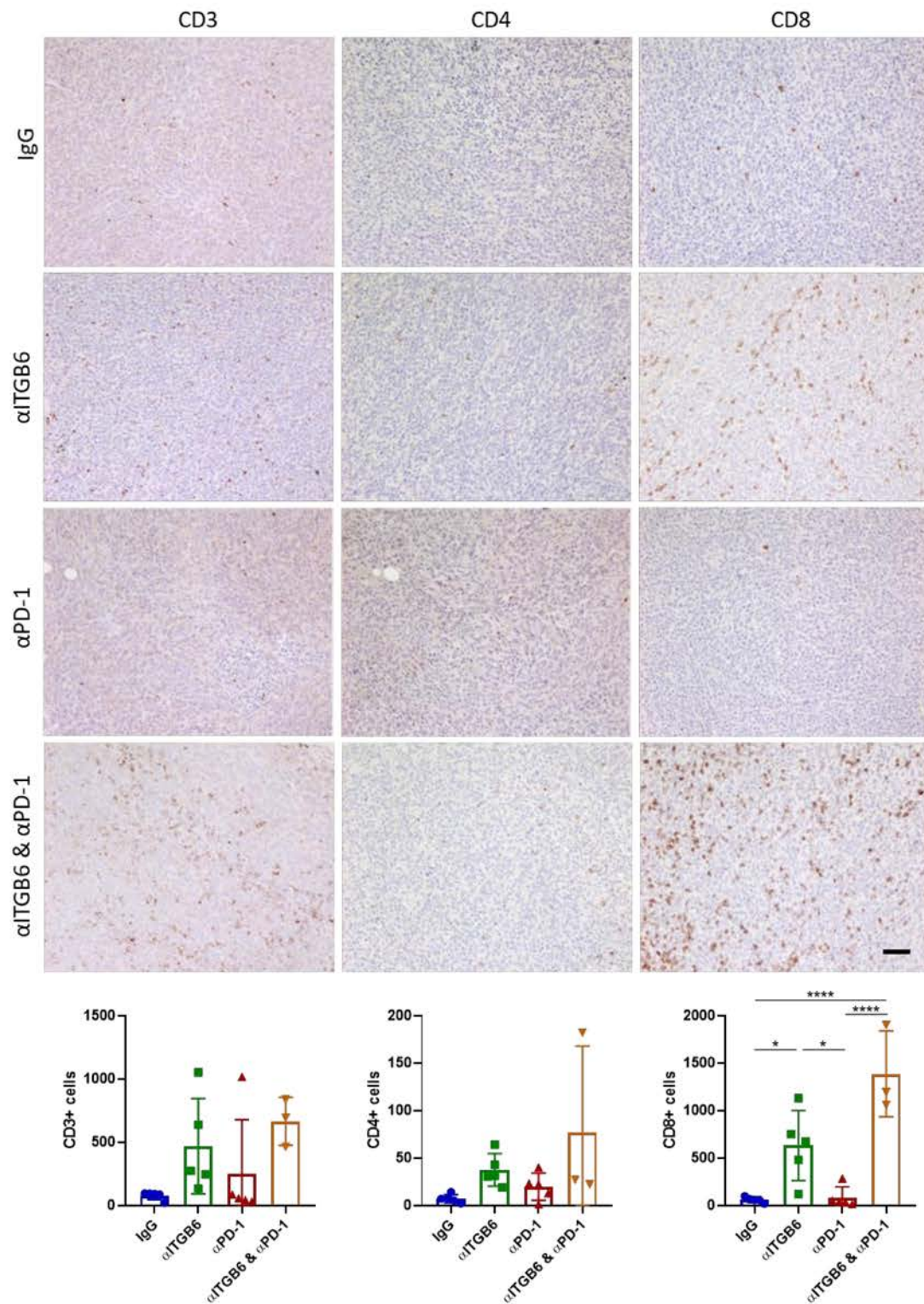


Fig. S6. IHC stainings of CD3, CD4 and CD8 in subcutaneous CT26-ITGB6 tumors treated with αITGB6 (6.8G6), αPD-1, αITGB6 (6.8G6) & αPD-1 or IgG control antibody. Representative images of IHC stainings (top) and quantification of the number of stained cells (bottom). Scale bar = 100 μm. Means and SDs are shown (n=3-5). One-way ANOVA with Tukey's post-hoc test was used to calculate statistical significance. *p < 0.05, **p < 0.01, ***p < 0.001, ****p < 0.0001.

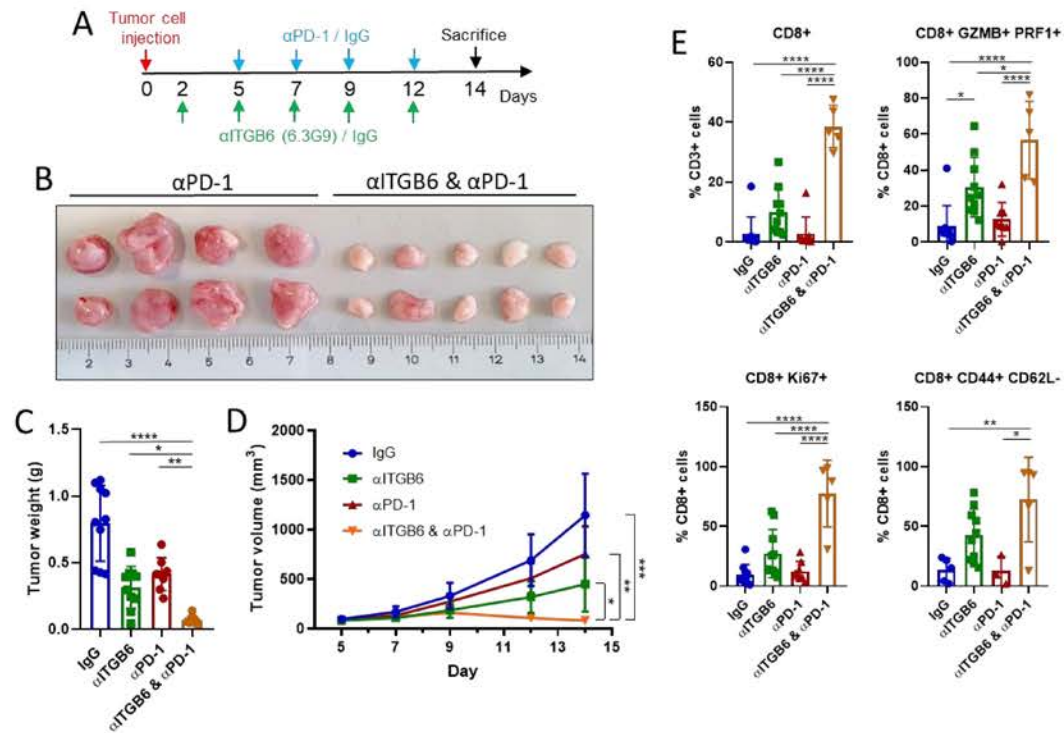


Fig. S7. (A) Experimental design of α ITGB6 (6.3G9) & α PD-1 antibody administration. (B) Subcutaneous CT26-ITGB6 tumors treated with α PD-1 or α ITGB6 (6.3G9) & α PD-1. (C) Tumor weight of subcutaneous CT26-ITGB6 tumors treated with α ITGB6 (6.3G9), α PD-1, α ITGB6 (6.3G9) & α PD-1 or IgG control. (D) Tumor volume development of subcutaneous CT26-ITGB6 tumors treated with α ITGB6 (6.3G9), α PD-1, α ITGB6 (6.3G9) & α PD-1 or IgG control. (E) Flow cytometry analysis of CD8+ T-cells in CT26-ITGB6 tumors treated with α ITGB6 (6.3G9), α PD-1, α ITGB6 (6.3G9) & α PD-1 or IgG control antibody. Means and SDs are shown (n=4-5 mice, 2 tumors per mouse). One-way ANOVA (C and E) and two-way ANOVA (D) with Tukey's post-hoc test was used to calculate statistical significance. *p < 0.05, **p < 0.01, ***p < 0.001, ****p < 0.0001.

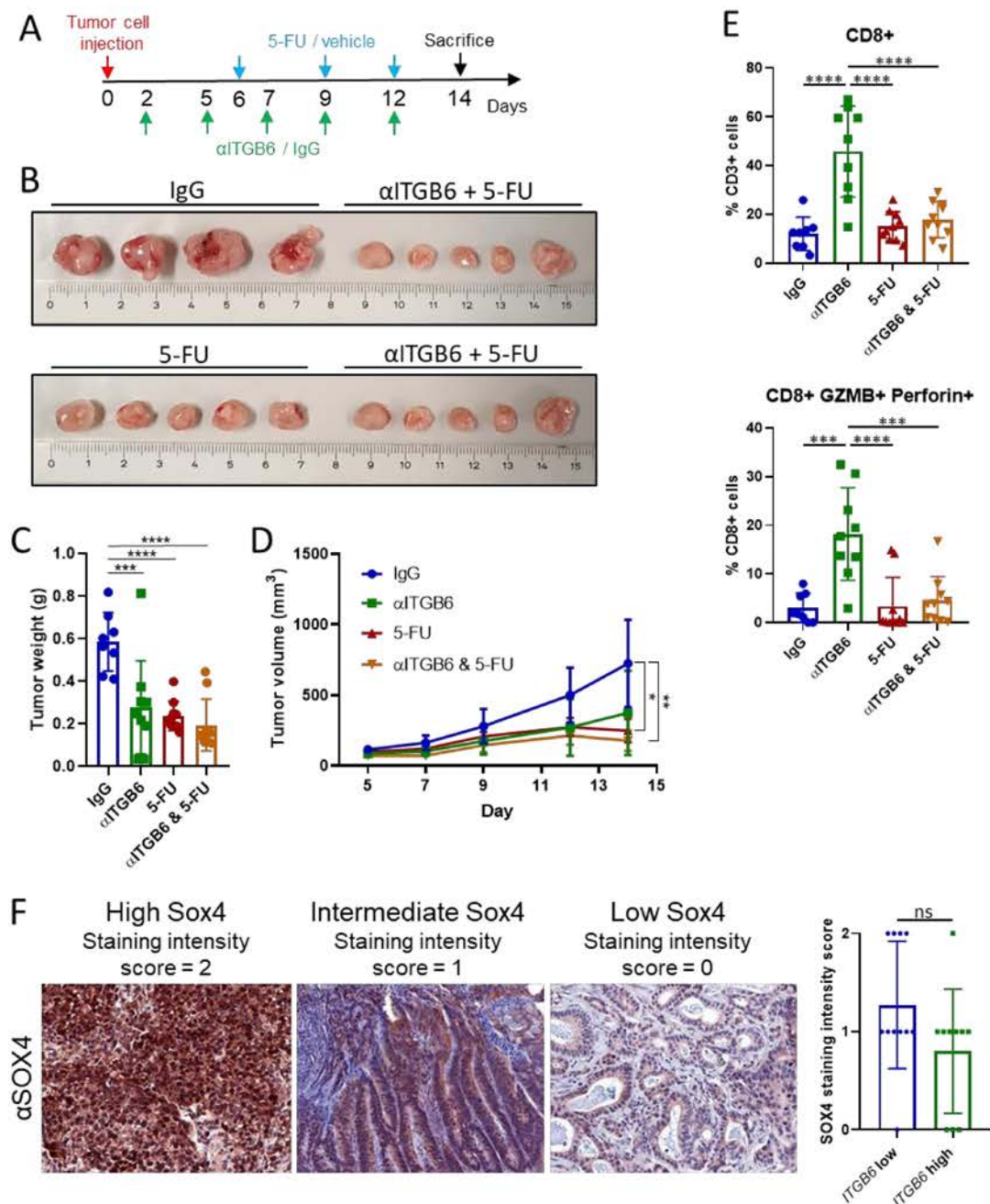


Fig. S8. (A) Experimental design of αITGB6 (6.8G6) & 5-FU treatment administration. (B) Representative image of subcutaneous CT26-ITGB6 tumors treated with 5-FU, αITGB6 & 5-FU or IgG control. (C) Tumor weight of subcutaneous CT26-ITGB6 tumors treated with αITGB6, 5-FU, αITGB6 & 5-FU or IgG control. (D) Tumor volume development of subcutaneous CT26-ITGB6 tumors treated with αITGB6, 5-FU, αITGB6 & 5-FU or IgG control. (E) Flow cytometry analysis of CD8+ T-cells in CT26-ITGB6 tumors treated with αITGB6, 5-FU, αITGB6 & 5-FU or IgG control antibody. (F) IHC staining of human CRC tumors with high (ITGB6: 40-ΔCt > 31.9) or low (ITGB6: 40-ΔCt < 28.4) ITGB6 mRNA expression. Representative images of staining intensity (left) and quantification of staining intensity scores (right). Means and SDs are shown (n=4-5 mice, 2 tumors per mouse). One-way ANOVA (C and E), two-way ANOVA (D) and Mann-Whitney test (F) was used to calculate statistical significance. *p < 0.05, **p < 0.01, ***p < 0.001, ****p < 0.0001

	Patients, n = 343
Gender	
Males	201 (58.6 %)
Females	142 (41.4 %)
Age	
Median	70 years
Range	24 – 96 years
ITGB6	
40- Δ Ct \leq 30	109
40- Δ Ct > 30	234
UICC stages	
Stage I	75 (21.87 %)
Stage II	117 (34.11 %)
Stage III	88 (25.66 %)
Stage IV	63 (18.37 %)
Histopathological grading	
Low grade (G ₁ /G ₂)	226 (65.89)
High grade (G ₃ /G ₄)	117 (34.11)

Table S1: Clinical characteristics of the colon carcinoma patients included in the analysis of ITGB6 expression

Supplier	Clone	Antigen	Fluorochrome
BioLegend	17A2	CD3	BV785
BD Biosciences	GK1.5	CD4	BV711
BioLegend	MP6-XT22	TNF α	BV650
BioLegend	30-F11	CD45	BV510
BioLegend	QA16A02	Granzyme B	PerCP-Cy5.5
BioLegend	XMG1.2	IFN γ	PE-Cy7
Thermo Fisher Scientific	RA3-6B2	B220/CD45R	PE-Cy5
BD Biosciences	53-6.7	CD8	PE-CF594
BioLegend	S16009B	Perforin	APC
Thermo Fisher Scientific	4B10	Tbet	PE
BioLegend	RM4-5	CD4	BV650
BioLegend	29F.1A12	PD-1	APC
BioLegend	MEL-14	CD62L	FITC
BioLegend	UC10-4B9	CTLA4	PE-Cy7
Thermo Fisher Scientific	IM7	CD44	APC
BioLegend	16A8	Ki67	AF700

Table S2: Flow cytometry antibodies

References

1. Naschberger E, Liebl A, Schellerer VS, et al. Matricellular protein SPARCL1 regulates tumor microenvironment-dependent endothelial cell heterogeneity in colorectal carcinoma. *J Clin Invest* 2016;126:4187-4204.
2. Klingler A, Regensburger D, Tenkerian C, et al. Species-, organ- and cell-type-dependent expression of SPARCL1 in human and mouse tissues. *PLoS One* 2020;15:e0233422.